Exciplex Emission and Room Temperature Phosphorescence from Donor-Acceptor Based Solvent-free Organic Liquid Hybrids

Vivek Chandrakant Wakcahure,[a,b] Sairam D. Veer,[a,b] Aakash D. Nidhankar,[a,b] Goudappagouda,[a,b] Rashmi Nayak,[a,b] Kiran Asokan,[a,b] Sapna Ravindranathan,[b,c] Sukumaran Santhosh Babu*[a,b]

a. Organic Chemistry Division, National Chemical Laboratory (CSIR-NCL), Pune-411008, India.

b. Academy of Scientific and Innovative Research (AcSIR), Ghaziabad-201002, India.

c. Central NMR Facility, National Chemical Laboratory (CSIR-NCL), Dr. Homi Bhabha Road, Pune-411008, India

Table of Contents

1. Experimental

Materials

All chemicals, 12-Tricosanone, 1-Bromo-2-ethylhexane, Hexane-1-amine, 1-Bromo hexane, Carbazole, 1,8-Naphthalic anhydride, Naphthalene-1,4,5,8-tetracarboxylic dianhydride, Ammonium acetate, Sodium cyanoborohydride, Hydrochloric acid, were purchased from commercial suppliers and used as such without further purification. Solvents such as N,N-dimethylformamide, dichloromethane, methanol, diethyl ether, n-hexane, petroleum ether, ethyl acetate were distilled before use.

Thin-layer chromatography was carried out using Aluchrosep Silica Gel 60/UV254 purchased from Merck Specialities Pvt Ltd and visualized either by UV Fluorescence or by iodine chamber. Column chromatography was performed using silica gel (100-200 mesh). The bed was made using 60-120 mesh silica purchased from Spectrochem Pvt. Ltd. India, and mixtures of DCM-PET used for elution were distilled before use.

General

All the reactions were carried out in oven-dried round bottom flasks under an argon atmosphere unless otherwise mentioned. The ^{1}H, ^{13}C NMR spectra were recorded at Bruker-400 MHz NMR spectrometer instrument. The chemical shift values for ^{1}H (TMS as internal standard) and ^{13}C NMR are recorded in CDCl$_3$. The value of the coupling constant (J) is stated in Hertz (Hz). High-resolution mass spectra (HRMS) were recorded on a Thermo Scientific Q-Exactive, Accela 1250 pump. UV-Vis absorption spectra were recorded on SHIMADZU UV-3600 plus UV-VIS-NIR spectrophotometer, while all emission spectra were performed using PTI Quanta Master™ Steady State Spectrofluorometer. Fluorescence lifetimes were measured by time-correlated single-photon counting (TCSPC), using a spectrofluorometer (Horiba Scientific), and an LED excitation source is 374 nm. The quality of the fit has been judged by fitting parameters such as χ^2 (<1.2) as well as visual inspection of the residuals. Phosphorescence spectra were recorded using Fluorolog-3 HORIBA JOBIN VYON spectrophotometer. DSC Q 10 differential scanning calorimeter connected to Q Series PCA (TA Instruments, USA) was used to determine the phase transition temperatures of the molecule. TGA data were collected in METTLER TOLEDO, TGA/SDTA851 instrument. The rheology experiment was carried out using an MCR dynamic oscillatory Cup and Bob Frequency Sweep at 20 ^{o}C using about 5 ml of the liquid samples. Luminescence quantum yield was measured using a Quanta-Phi 6″ model F-3029. HPLC analysis is performed on

Agilent 1260, Infinity Series using normal (Zweite silica, 5 μm, 4.6 x 250 mm) and reverse-phase (Shimadzu, Shim-pack GIST, 5 μm, C18, 4.6 x 250 mm) columns.

Preparation of EL and RTPL

The donor and acceptor with different equivalents in glass vials (1.5 mL) were either stirred well with a spatula or heated gently to become a homogeneous mixture.

UV-VIS Spectra of Neat Liquids

UV-Vis spectra of all neat liquids were recorded in the transmittance mode, and the samples were prepared by making a uniform, transparent coating of 5 mg sample on a 1 x 1 cm^2 area of quartz plate. The consistency of each spectrum was confirmed by repeated trials.

NMR Experiments

All the NMR spectra in the neat condition were recorded by placing the compounds (~ 200 mg) in a 3 mm NMR tube and inserting it in an outer 5 mm NMR tube containing *DMSO-d_6* as an external lock. The actual ratios of donor and acceptor were estimated by integrating peak areas of the aromatic protons. Solution state NMR was recorded by dissolving 12 mg of the compound in 0.6 mL of solvent.

Phosphorescence Experiments

All phosphorescence experiments have been done in the air by keeping the same experimental parameters. The window of maximum delay after flash for phosphorescence measurements was kept 0.5 ms.

2. Synthesis
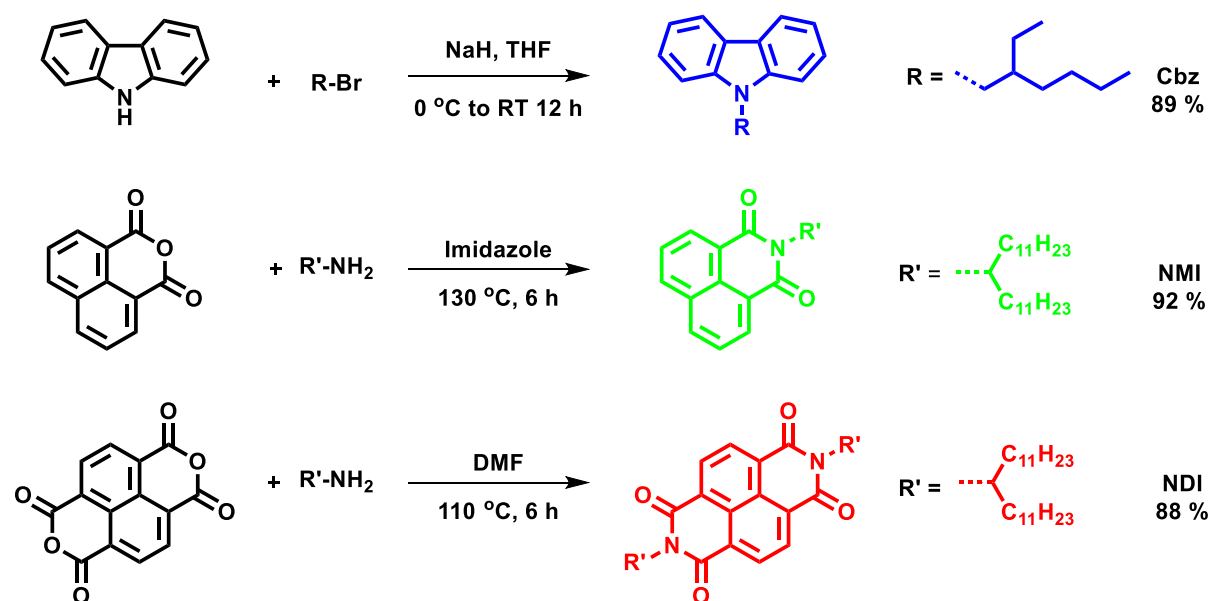
Scheme S1. Synthesis of **Cbz**, **NMI**, and **NDI**.

Synthesis of 9-(2-ethylhexyl)-9H-carbazole (Cbz)[S1]
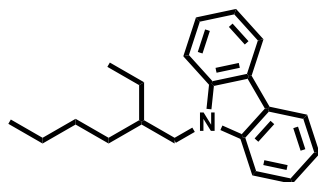
In a two-neck round, the bottom flask was placed carbazole (1 eq.), bromoalkane (1.1 eq.), KOH (1.1 eq.), TBAB (tetrabutylammonium bromide, 0.1 eq.), and DMF (50 mL). The obtained mixture was stirred at 70 °C for 24 hours. After cooling down, water and chloroform were added (each 100 mL) and thoroughly shaken. The organic layer was separated, and the inorganic layer was extracted again with chloroform (100 mL). Combined organic extracts were washed with water (100 mL), two times with NaCl saturated solution (2 x 100 mL), and finally dried with anhydrous Na_2SO_4. Yellowish oil was subjected to column chromatography on silica gel, using petroleum ether as a mobile phase to get the product.

Nature and Yield: colourless liquid, 89%.

^{1}H-NMR: (400 MHz, CDCl$_3$, 25 °C): δ = 8.12-8.07 (2H, m), 7.50-7.36 (4H, m), 7.25-7.17 (2H, m), 4.19-4.17 (4H, m), 2.12-2.04 (1H, m), 1.42-1.24 (8H, m), 1.37-1.34 (8H, m), 0.93-0.82 (6H, m) ppm.

^{13}C-NMR: (100 MHz, CDCl$_3$, 25 ^{o}C): δ = 140.91, 125.89, 122.76, 120.24, 118.63, 108.92, 47.38, 39.38, 31.00, 28.81, 24.39, 23.04, 14.01, 10.89 ppm.

HR-MS: calcd. for C$_{20}$H$_{25}$N = 279.1987, found 279.1982.

Tricosan-12-amine
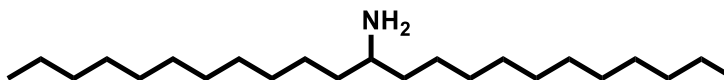
1,2-Tricosanone, NH$_4$OAc and NaBH$_3$CN were dissolved in 40 mL methanol (HPLC grade) and stirred at RT for 56 h (3 days). Then the reaction was quenched by adding con. HCl dropwise. The solution was then concentrated with the rotatory evaporator. The solid thus obtained is dispersed in 250 mL of water and adjusted to pH = 10 with KOH. The obtained latex solution was evaporated by 150 mL of CH$_2$Cl$_2$ and then 100 mL again. The pale yellow oil was obtained by concentrating the CH$_2$Cl$_2$ solution and used as such for the next step without further purification.

Synthesis of 2-(Tricosan-12-yl)-1H-benzo[de]isoquinoline-1,3(2H)-dione (NMI)[S2]
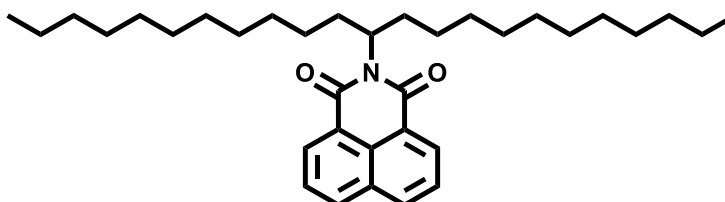
Tricosan-12-amine (1.05 eq.) and 1,8-naphthalic anhydride (1 eq.) were heated in imidazole (10 g) for 6 hours at 130 ^{o}C, subsequently cooled, and while still warm combined with a 2 M HCl followed by extraction with CH$_2$Cl$_2$ twice. The combined organic phases were dried with (Na$_2$SO$_4$), the solvent was removed by vacuum, and the product was purified by column chromatography.

Nature and Yield: pale yellow liquid, 92%.

^{1}H NMR: (CDCl$_3$, 400 MHz, 25 ^{o}C): δ = 8.60-8.57 (2H, m), 8.19 (2H, d, J = 8.3 Hz), 7.76 (2H, t, J = 8.3 Hz), 5.25-5.13 (1H, m), 2.30-2.15 (2H, m), 1.91-1.75 (2H, m), 1.28-1.20 (36H, m), 0.86 (6H, t, J = 6.18 Hz) ppm.

^{13}C NMR: (CDCl$_3$, 100 MHz, 25.0 $^\circ$C): δ = 165.4, 164.3, 133.5, 131.5, 131.5, 130.8, 128.3, 126.9, 123.4, 123.7, 54.4, 32.4, 31.8, 29.5, 29.5, 29.2, 26.9, 22.6, 14.1 ppm.

HRMS: calcd. for $C_{35}H_{53}NO_2^+$ = 519.4076, found 519.4071.

Synthesis of 2,7-Di(tricosan-12-yl)benzo[lmn][3,8]phenanthroline-1,3,6,8(2H,7H)-tetraone (NDI)[S3]
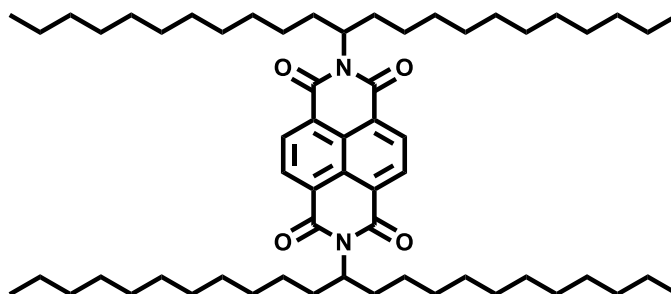
Naphthalene-1,4,5,8-tetracarboxylic dianhydride (1 eq.) and tricosan-12-amine (2.5 eq.) were suspended in DMF (20 mL) in 100 mL round bottom flask. The reaction mixture was stirred for 6 h at 140 °C. The progress of the reaction was monitored by TLC. After completion of the reaction, the reaction mixture was allowed to cool to RT, and it was quenched by the addition of hydrochloric acid (2N, 40 mL). The reaction mixture was extracted with dichloromethane (3 × 200 mL). The organic layer was dried over sodium sulfate, and the solvent was removed under reduced pressure. The crude product was purified by silica gel column chromatography by using 50% dichloromethane in petroleum ether as eluent. The combined organic layer was concentrated under reduced pressure and dried under vacuum to get the product.

Nature and Yield: solid, 88 %.

^{1}H-NMR (500 MHz, CDCl$_3$, 25 °C): δ = 8.73 (4H, s), 5.21-5.12 (2H, m), 2.24-2.17 (4H, m), 1.87-1.78 (4H, m), 1.33-1.19 (72H, m), 0.85 (12H, t, J = 6.8 Hz) ppm.

^{13}C-NMR (125 MHz, CDCl$_3$, 25 °C): δ = 164.1, 162.9, 131.3, 130.6, 126.8, 55.2, 32.3, 31.9, 29.6, 29.5, 29.3, 26.9, 22.7, 14.1 ppm.

HR-MS: calcd. for $C_{60}H_{98}N_2O_4$ = 910.7527, found 910.7521.
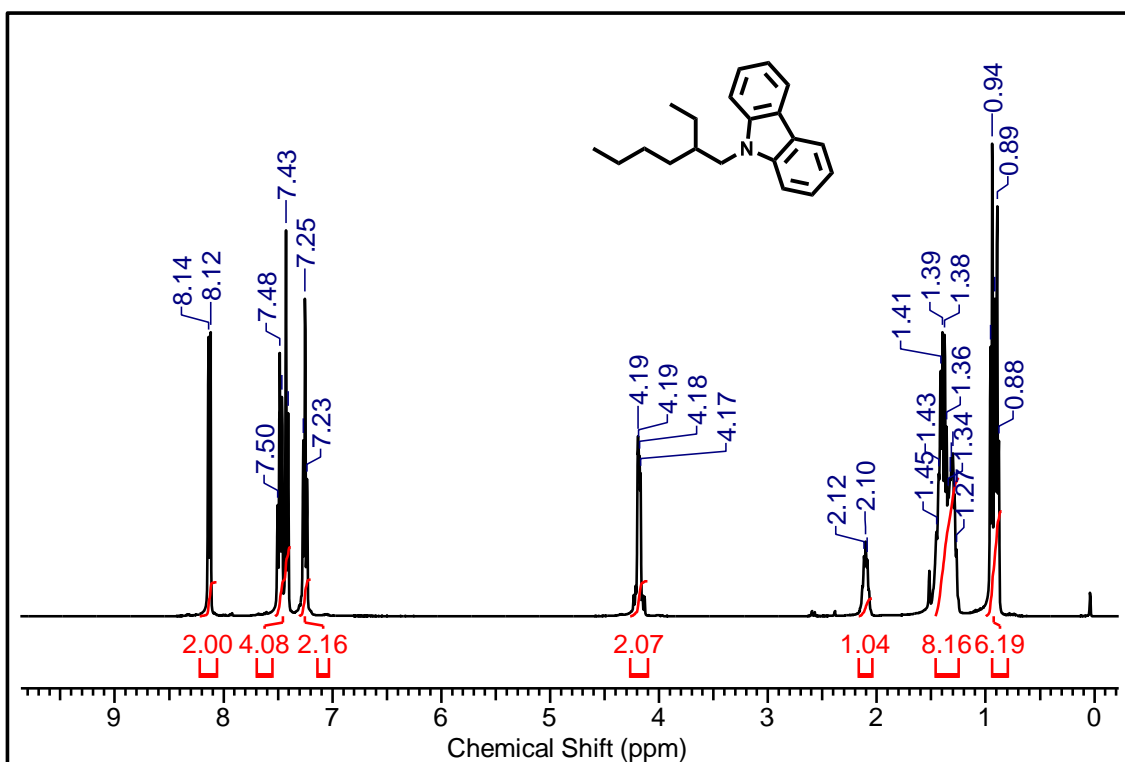
^{1}H NMR spectra of 9-(2-ethylhexyl)-9H-carbazole (**Cbz**).
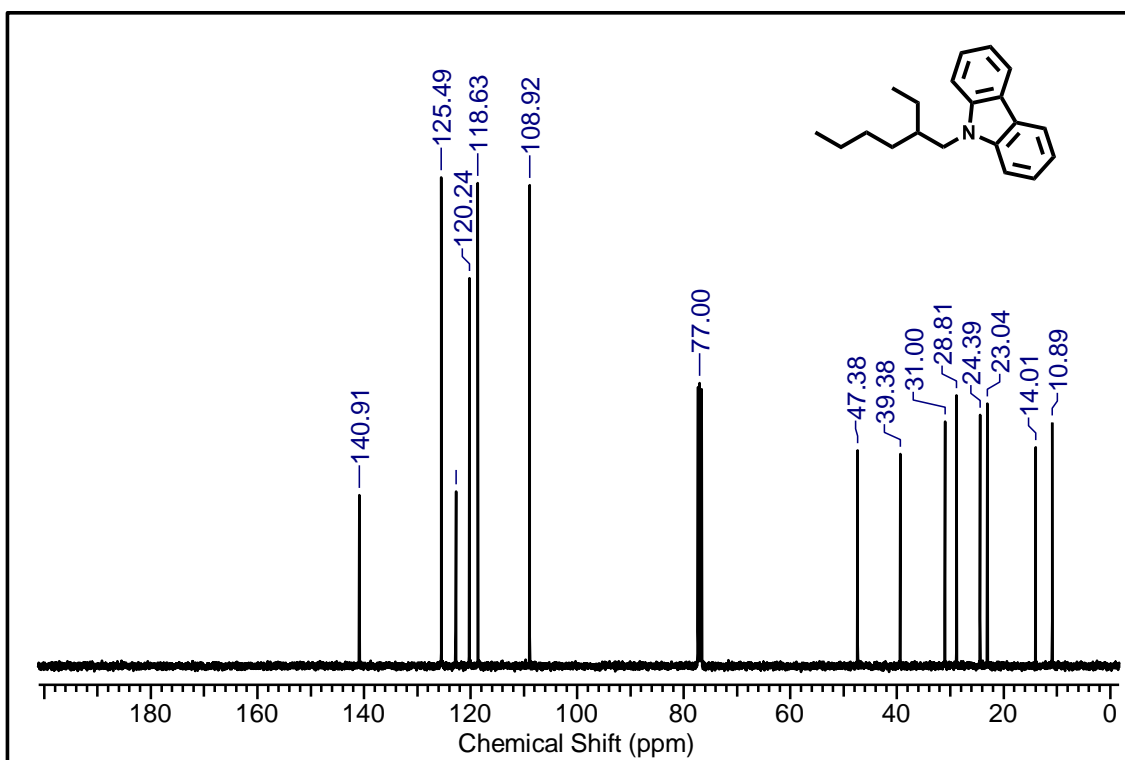
^{13}C NMR spectra of 9-(2-ethylhexyl)-9H-carbazole (**Cbz**).
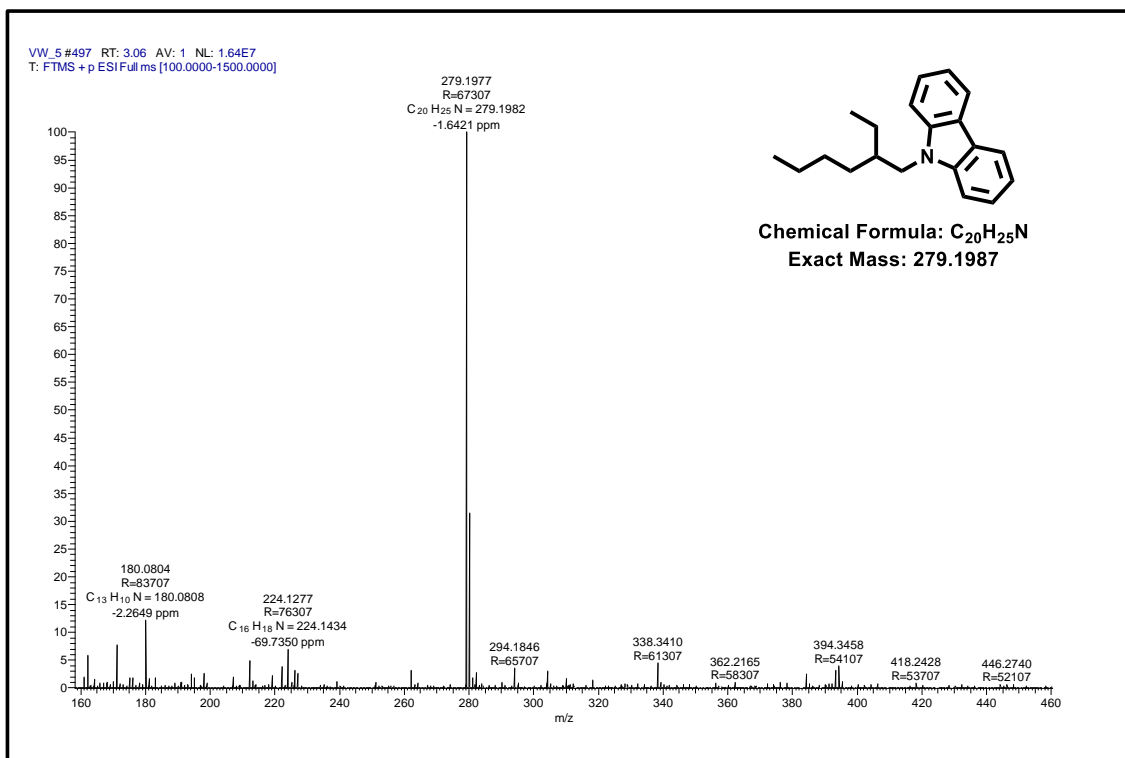
HRMS of 9-(2-ethylhexyl)-9H-carbazole (**Cbz**).
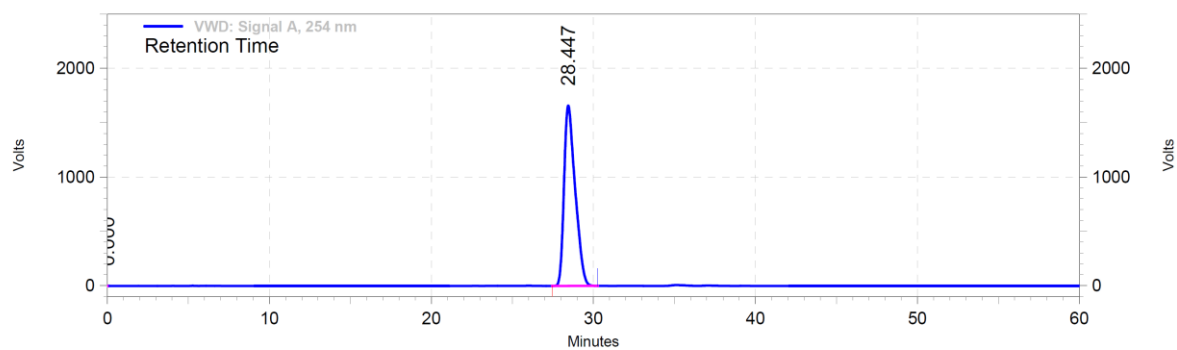
HPLC profile of **Cbz** (RT = 28.447), in acetonitrile:H_2O (90:10) by monitoring at 254 nm.
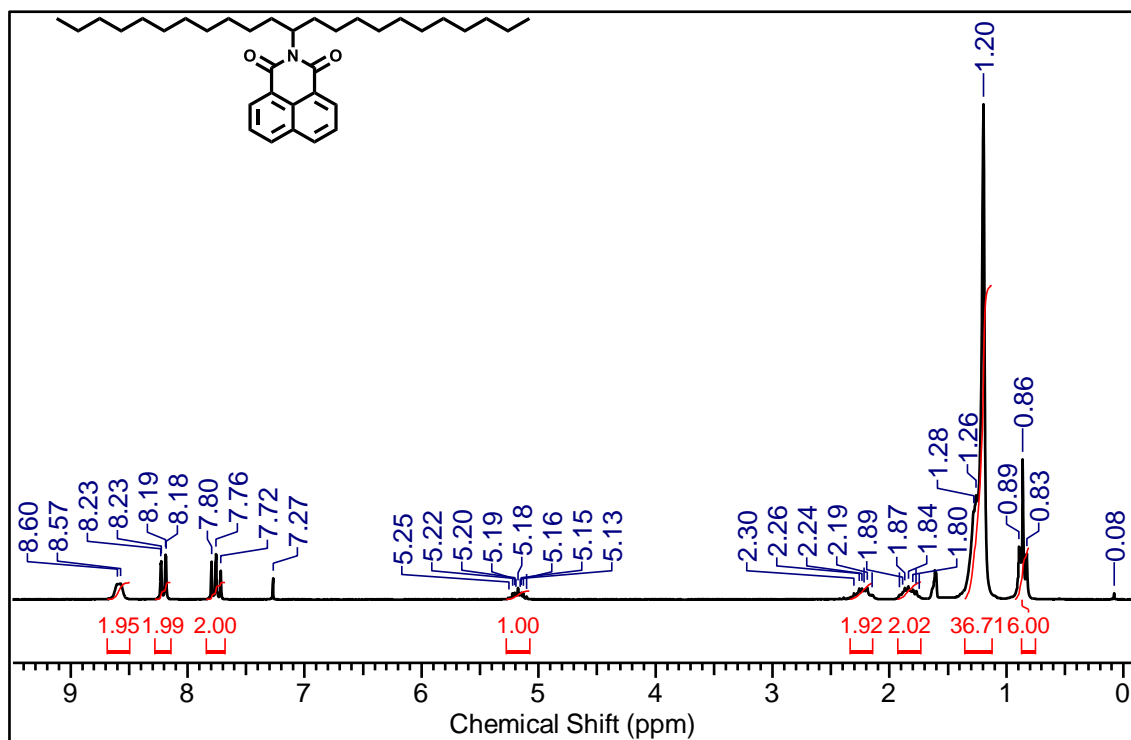
^{1}H NMR spectra of 2-(tricosan-12-yl)-1H-benzo[de]isoquinoline-1,3(2H)-dione (**NMI**).
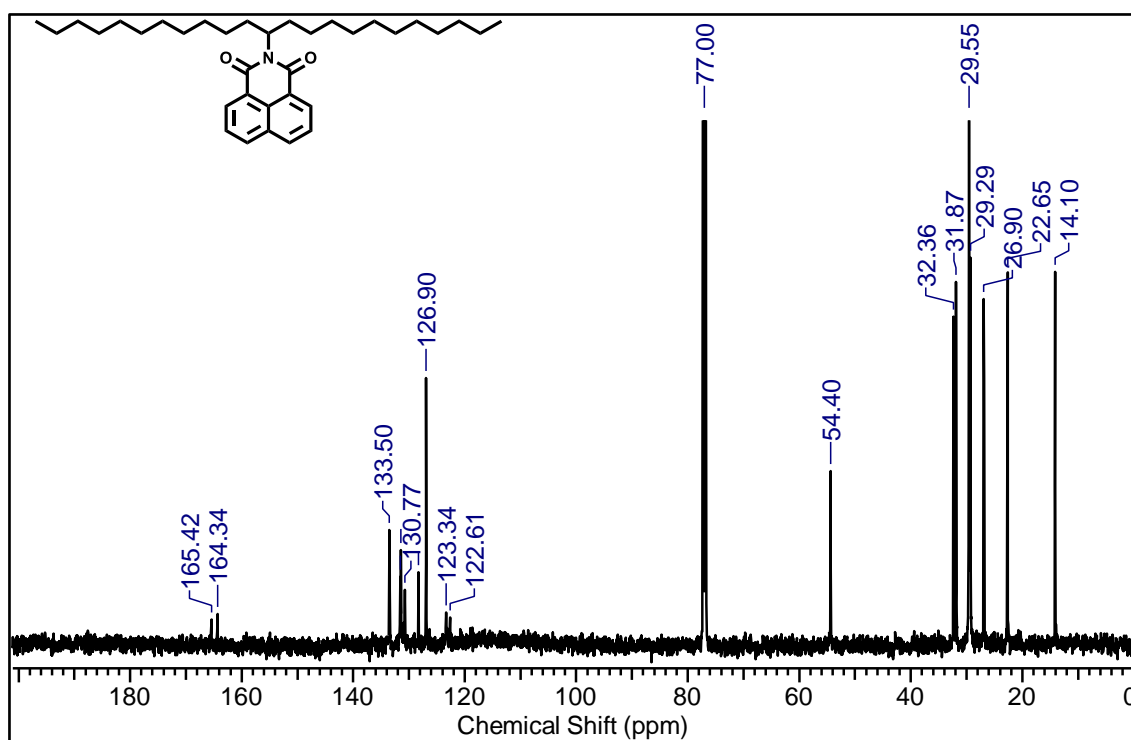
^{13}C NMR spectra of 2-(tricosan-12-yl)-1H-benzo[de]isoquinoline-1,3(2H)-dione (**NMI**).
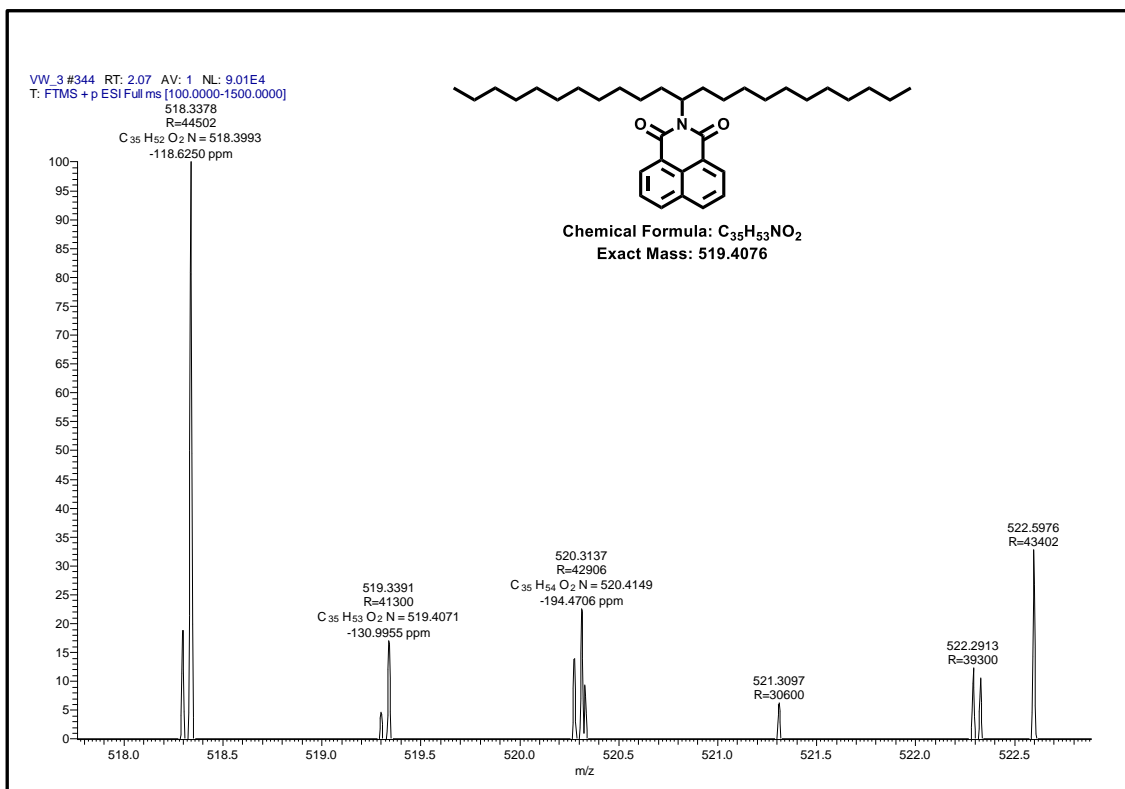
HRMS of 2-(tricosan-12-yl)-1H-benzo[de]isoquinoline-1,3(2H)-dione (**NMI**).
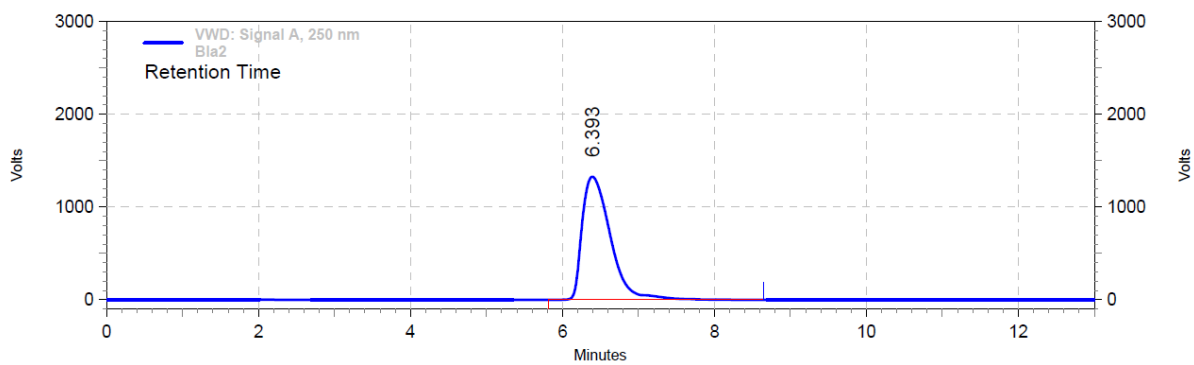
HPLC profile of **NMI** (RT = 6.393) in *n*-hexane:isopropanol (95:05) by monitoring at 254 nm.
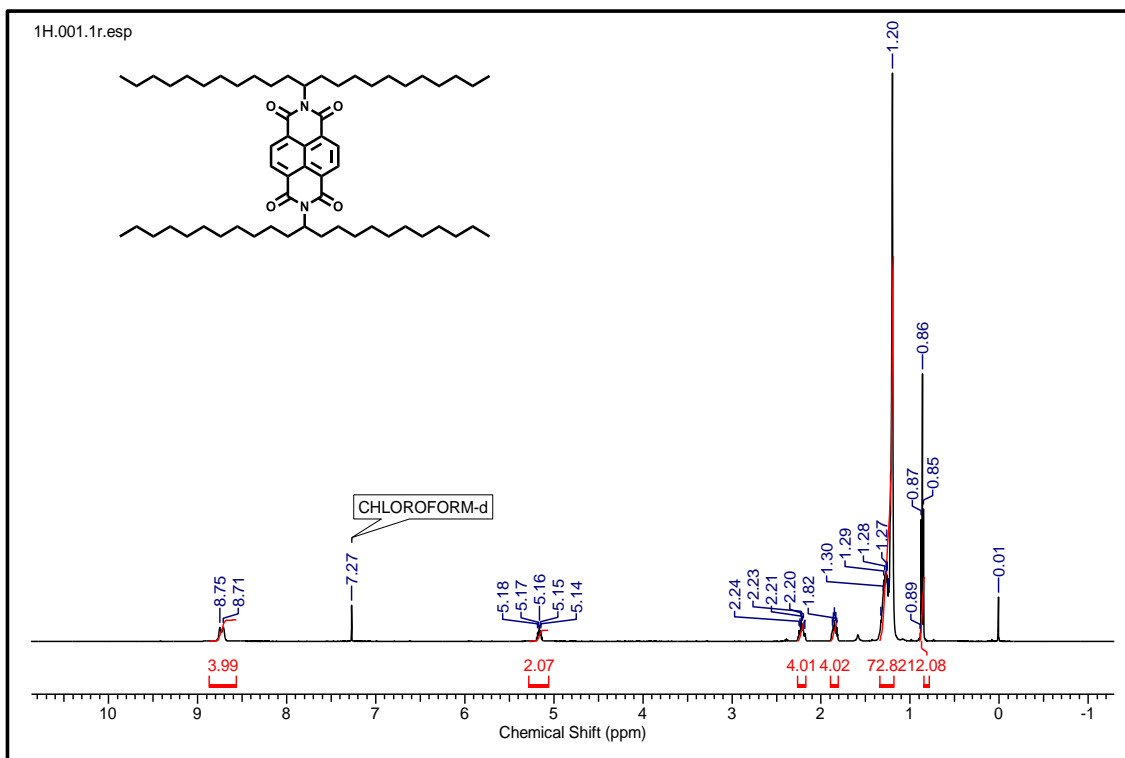
^{1}H NMR spectra of 2,7-di(tricosan-12-yl)benzo[lmn][3,8]phenanthroline-1,3,6,8(2H,7H)-tetraone (**NDI**).
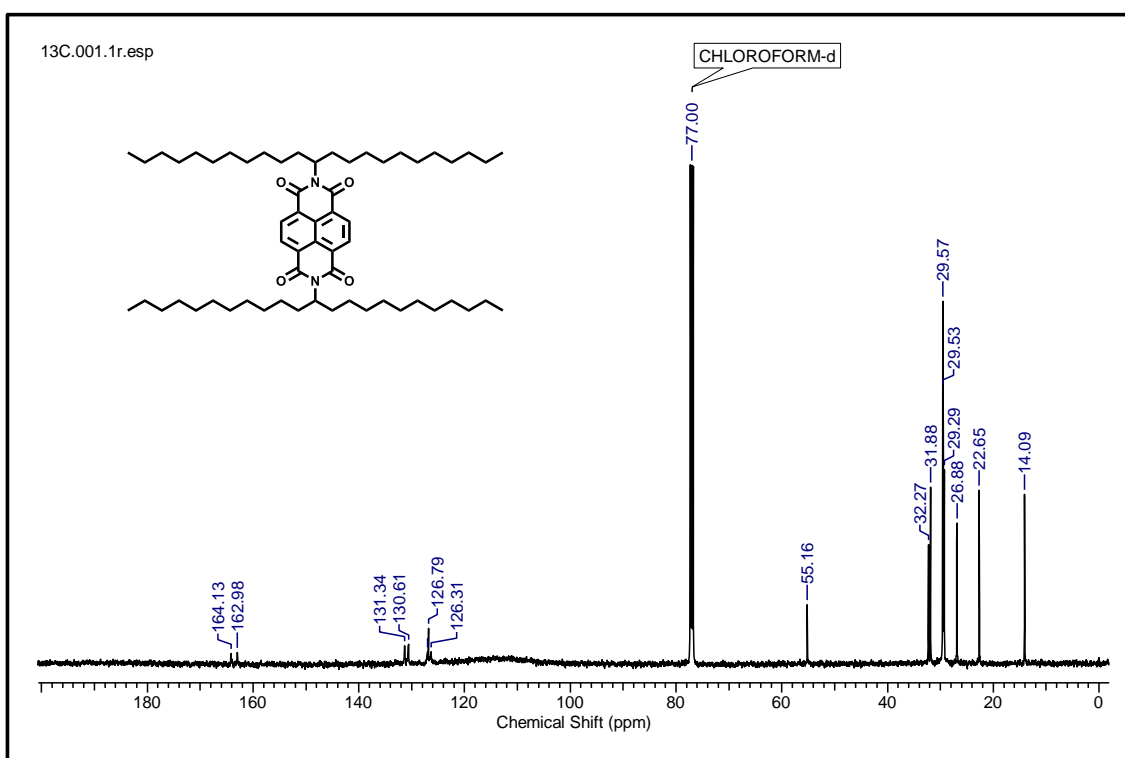
^{13}C NMR spectra of 2,7-di(tricosan-12-yl)benzo[lmn][3,8]phenanthroline-1,3,6,8(2H,7H)-tetraone (**NDI**).
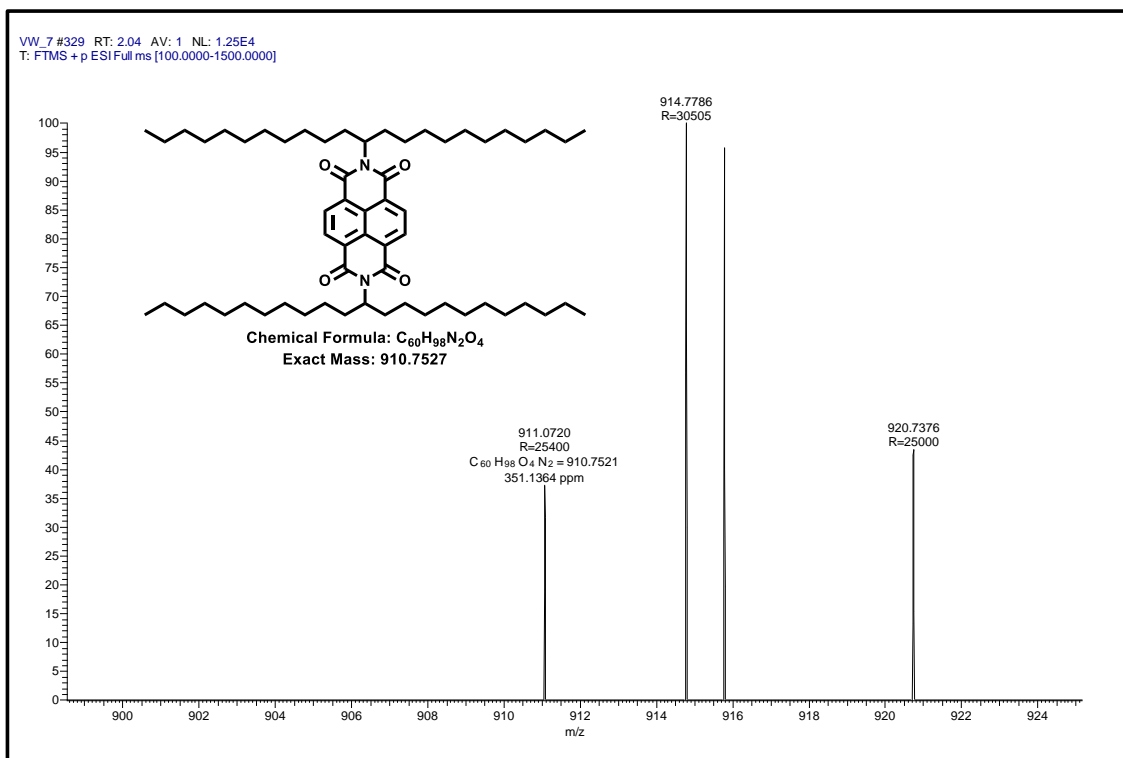
HRMS of 2,7-di(tricosan-12-yl)benzo[lmn][3,8]phenanthroline-1,3,6,8(2H,7H)-tetraone (**NDI**).
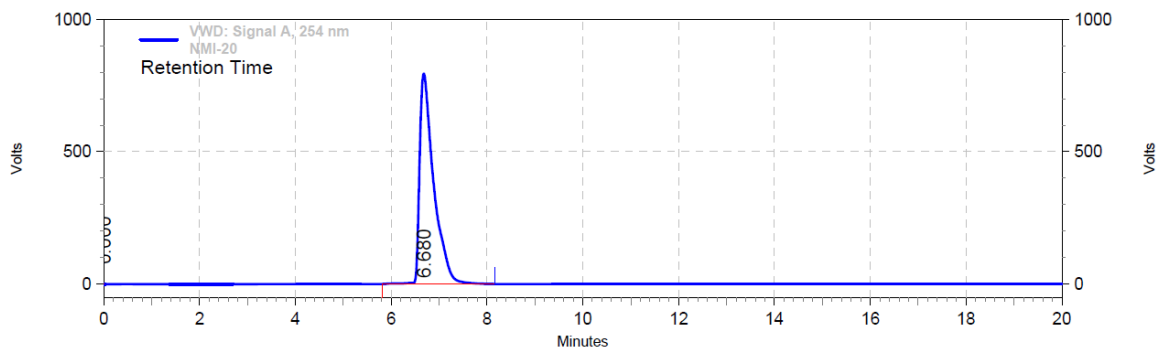
HPLC profile of **NDI** (RT = 6.68) in *n*-hexane:isopropanol (95:05) by monitoring at 254 nm.

CHN analysis of **Cbz**, **NMI**, **NDI**.

Compound	Chemical Formula:	Elemental Analysis: Theoretical			Elemental Analysis:Found		
		C	H	N	C	H	N
Cbz	$C_{20}H_{25}N$	85.97	9.02	5.01	86.21 (+0.24)	8.70 (-0.32)	5.40 (+0.39)
NMI	$C_{35}H_{53}NO_2$	80.87	10.28	2.69	80.91 (+0.04)	9.86 (-0.42)	3.17 (+0.48)
NDI	$C_{60}H_{98}N_2O_4$	79.07	10.84	3.07	79.56 (+0.49)	10.45 (-0.39)	2.71 (-0.36)

*The deviation of experimental value from the theoretical value is provided in bracket.

3. Figures
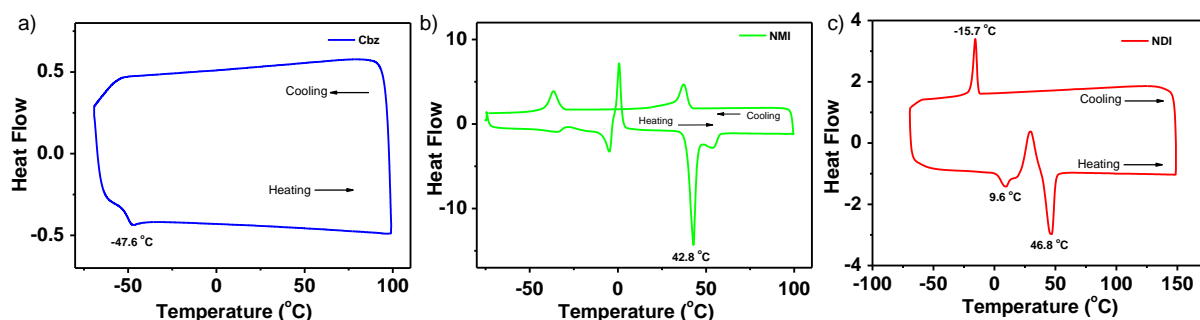
Figure S1. DSC thermograms in the heating trace at a scanning rate of 10 ˚C/min of a) **Cbz**, b) **NMI**, c) **NDI**.

*Cbz is a colourless free-flowing liquid at RT (30 ^{o}C) and exhibits a glass transition temperature (T_g, offset) around -47 ^{o}C as confirmed by differential scanning calorimetry (DSC). The acceptors **NMI** and **NDI** are low melting solids with a melting point (T_m) around 42 ^{o}C and 46 ^{o}C, respectively.*
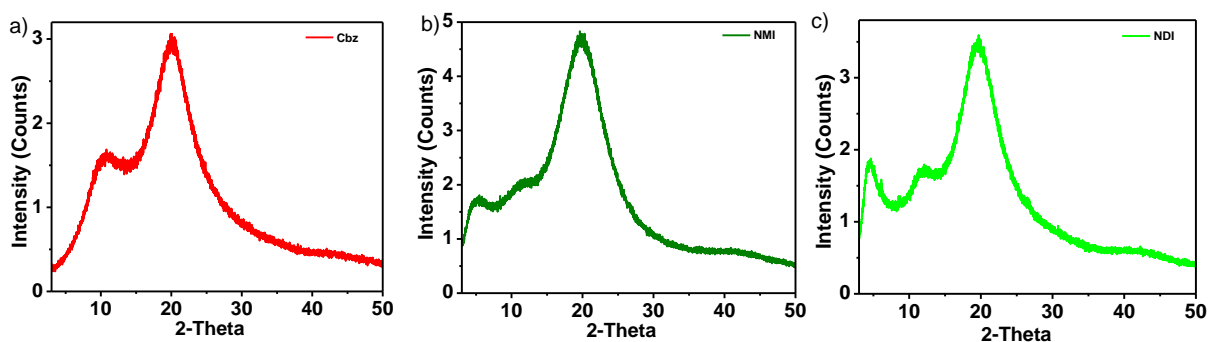
Figure S2. Comparison of PXRD pattern of **Cbz**, **NMI**, and **NDI**.

*The powder X-Ray diffraction (XRD) pattern shows that **Cbz, NMI,** and **NDI** lack crystalline ordering, however sharp peaks have been observed for other solid derivatives.*
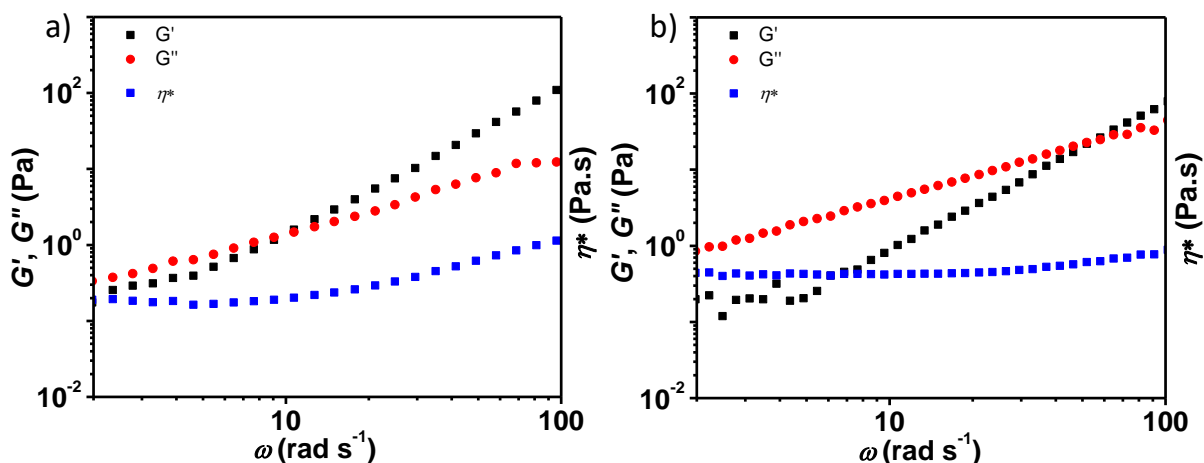
Figure S3. Variation of storage modulus (G') (■), loss modulus (G'') (●), and complex viscosity (η^*) (■) versus angular frequency on a double logarithmic scale, of a) **Cbz** and, b) **NMI**.

*Rheology experiments revealed that **Cbz** and **NMI** show viscous to elastic transition from low to high angular frequency. Both derivatives transform from solvent-free liquid to a semi-solid material with a gradual increase of frequency, indicating the characteristics of shear-hardening. Moreover, **CBz** shows a lower (~10 rad s^{-1}) modulus intersection point (G') compared to **NMI** (~20 rad s^{-1}).*
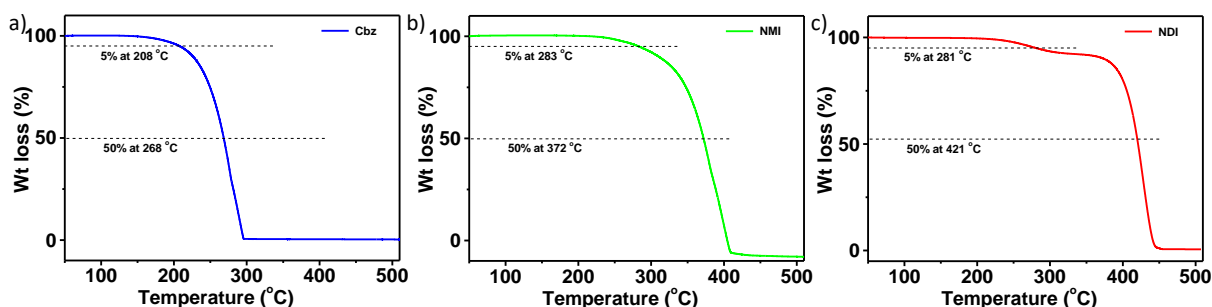
Figure S4. TGA of a) **Cbz**, b) **NMI**, and c) **NDI**.

*The thermal stability of all the molecules was checked by thermogravimetric analysis (TGA). It has been found that 5% weight loss was noticed at around 210 °C for **Cbz**. While for acceptors, it was varied as 283 °C (**NMI**), and 281 °C (**NDI**).*
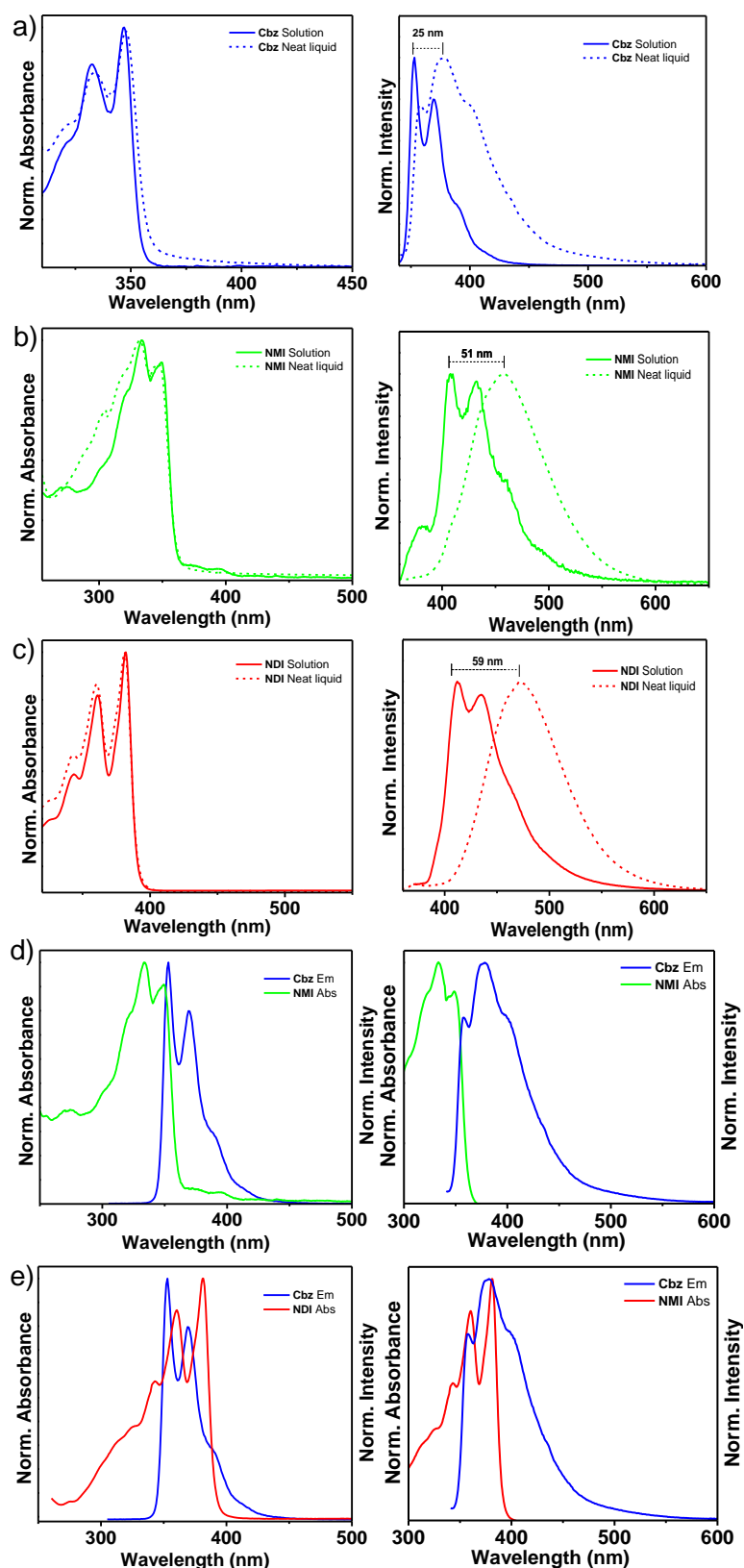
Figure S5. Normalized absorption (left) and emission (right) spectra of a) **Cbz**, b) **NMI**, c), and **NDI** in dichloromethane (solid line) and neat liquid thin film (dotted line), (λ_{ex} = 342 nm for **Cbz**; 350 nm for **NMI**; and 360 nm for **NDI**, C = 1x10^{-5} M, l = 1 mm). Spectral overlap between d) emission of **Cbz** and the absorption of **NMI** in solution (left) and neat liquid thin film (right) and e) emission of **Cbz** and the absorption of **NDI** in solution (left) and neat liquid thin film (right).
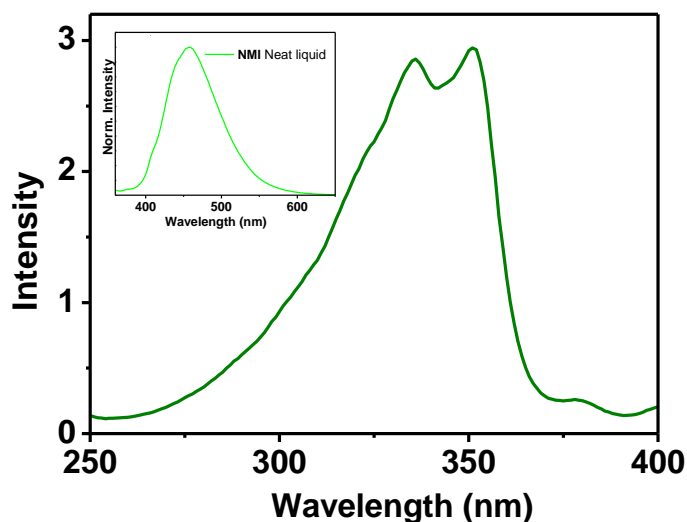
Figure S6. Excitation spectrum monitored at the major emission peak of **NMI** in the neat liquid state; insets show the corresponding emission spectra of neat liquid thin-film (λ_{ex} = 250-450 nm and λ_{mon} = 460 nm).
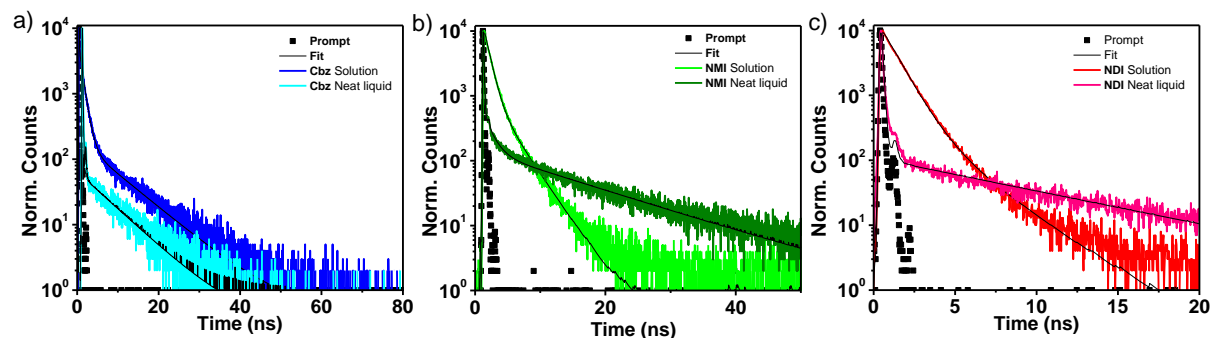
Figure S7. Emission lifetime decay profile of a) **Cbz** (λ_{mon} = 390 nm), b) **NMI** (λ_{mon} = 410 nm), c) **NDI** (λ_{mon} = 412 nm) in dichloromethane at 25 ˚C (λ_{ex} = 374 nm, C = 0.01 mM, l = 1 mm) and in neat liquid thin films at 25 ˚C, for **Cbz** λ_{mon} = 410 nm, **NMI** λ_{mon} = 460 nm, **NMI** λ_{mon} = 472 nm, λ_{ex} = 374 nm.
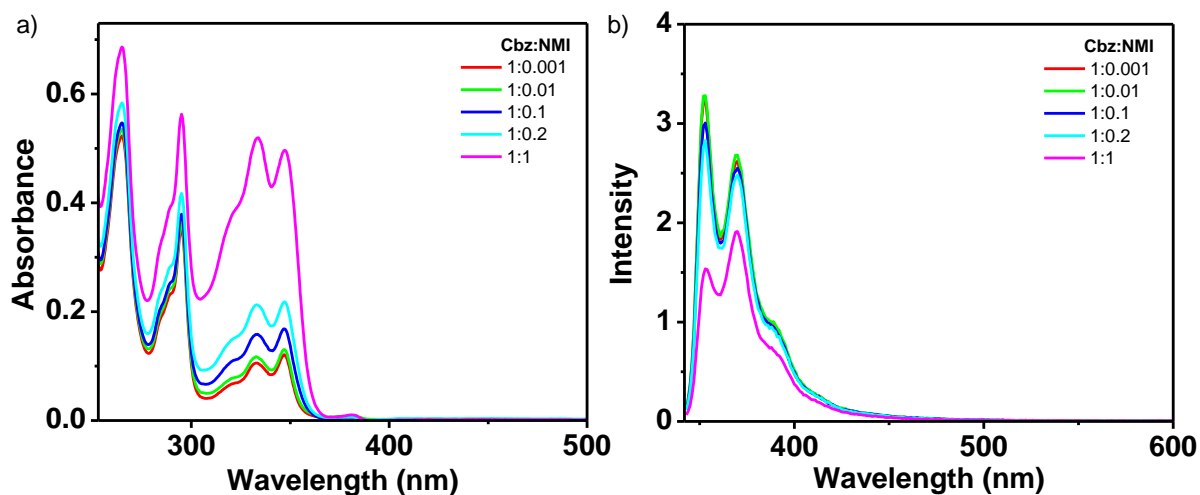
Figure S8. Variation of absorption and emission spectra of **Cbz**:**NMI** with an increasing equivalents of **NMI** in dichloromethane solution (l = 1 cm, C = 1x10^{-5} M, λ_{ex} = 333 nm).
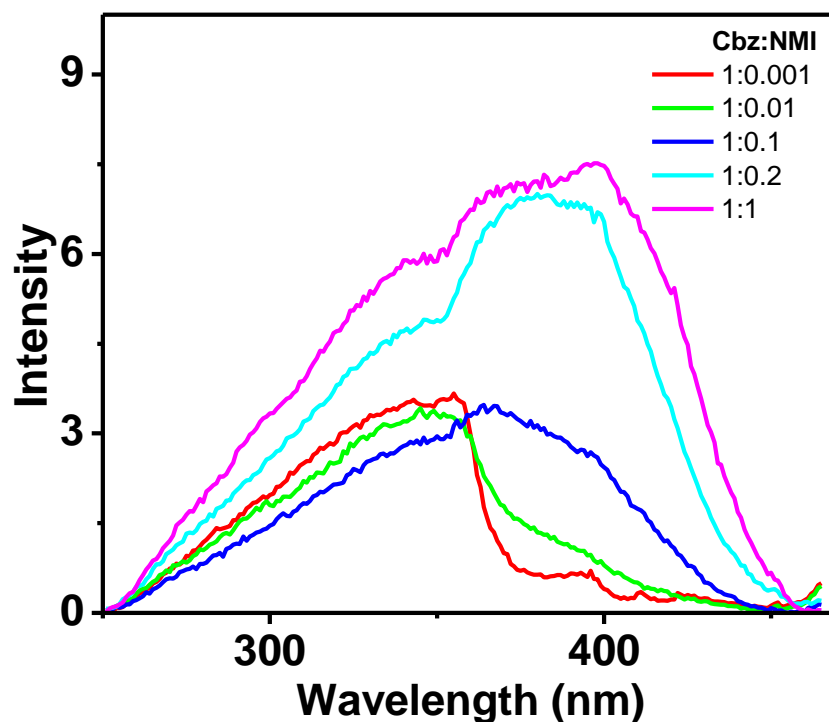
Figure S9. Variation of excitation spectra of **Cbz:NMI** with an increasing equivalents of **NMI** in the neat liquid thin film (λ_{ex} = 250-480 nm, λ_{mon} = 485 nm).
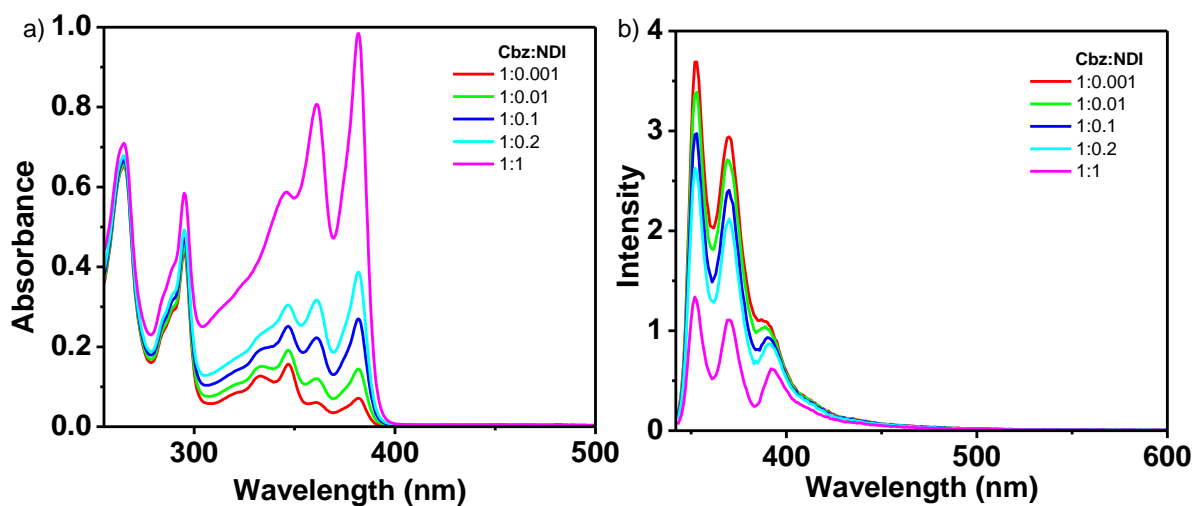
Figure S10. Variation of absorption and emission spectra of **Cbz:NDI** with an increasing equivalents of **NDI** in dichloromethane solution (l = 1 cm, C = 10^{-5} M, λ_{ex} = 333 nm).
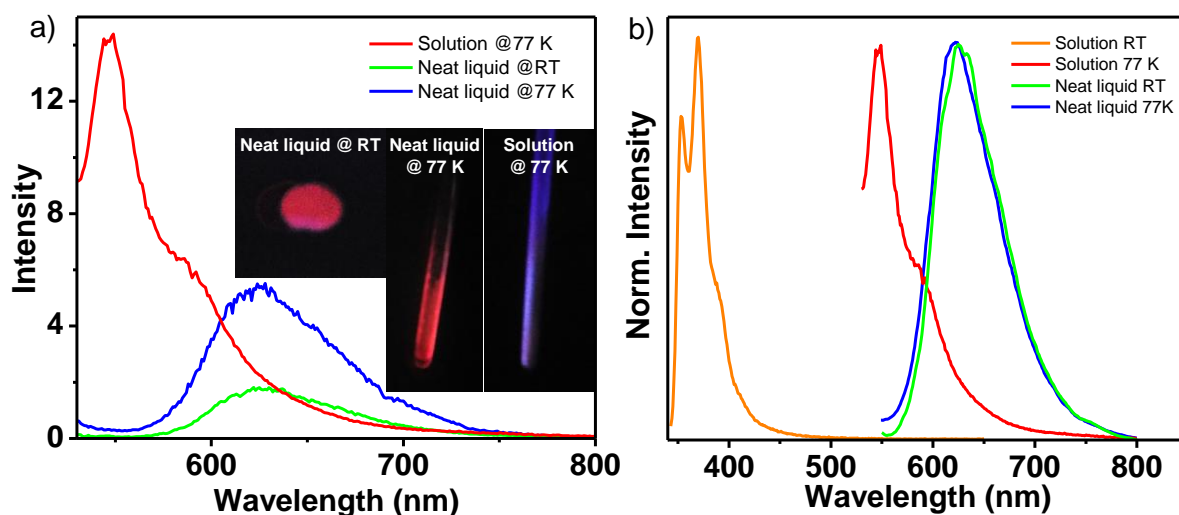
Figure S11. a) Comparison of the emission spectra of **Cbz:NDI** (1:1) in the solution at 77 K, neat liquid at RT and 77 K, inset shows the photographs and b) corresponding normalised spectra along with solution state emission at RT.
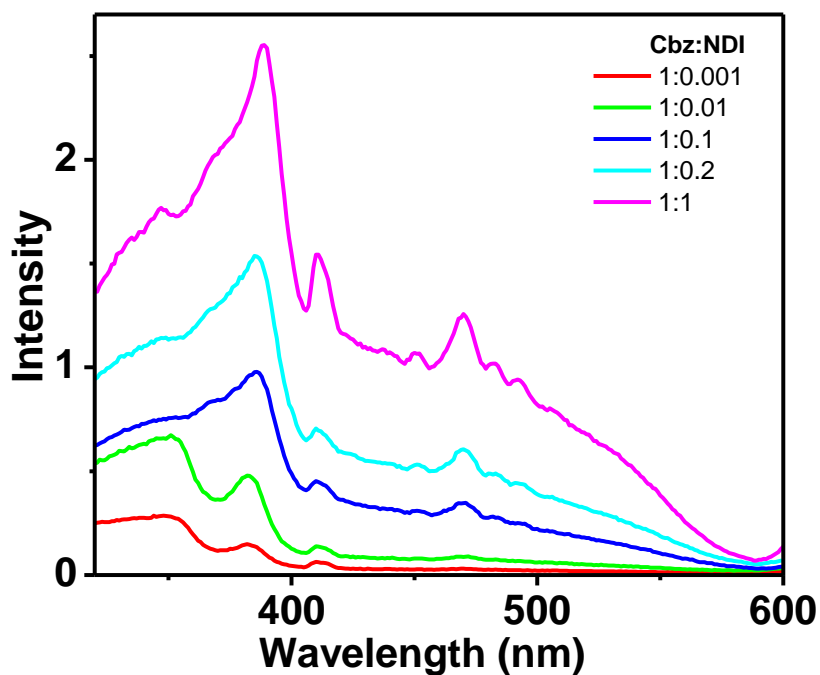
Figure S12. Variation of excitation spectra of **Cbz:NDI** with an increasing equivalents of **NDI** in the neat liquid thin film (λ_{ex} = 320-600 nm, λ_{mon} = 620 nm).
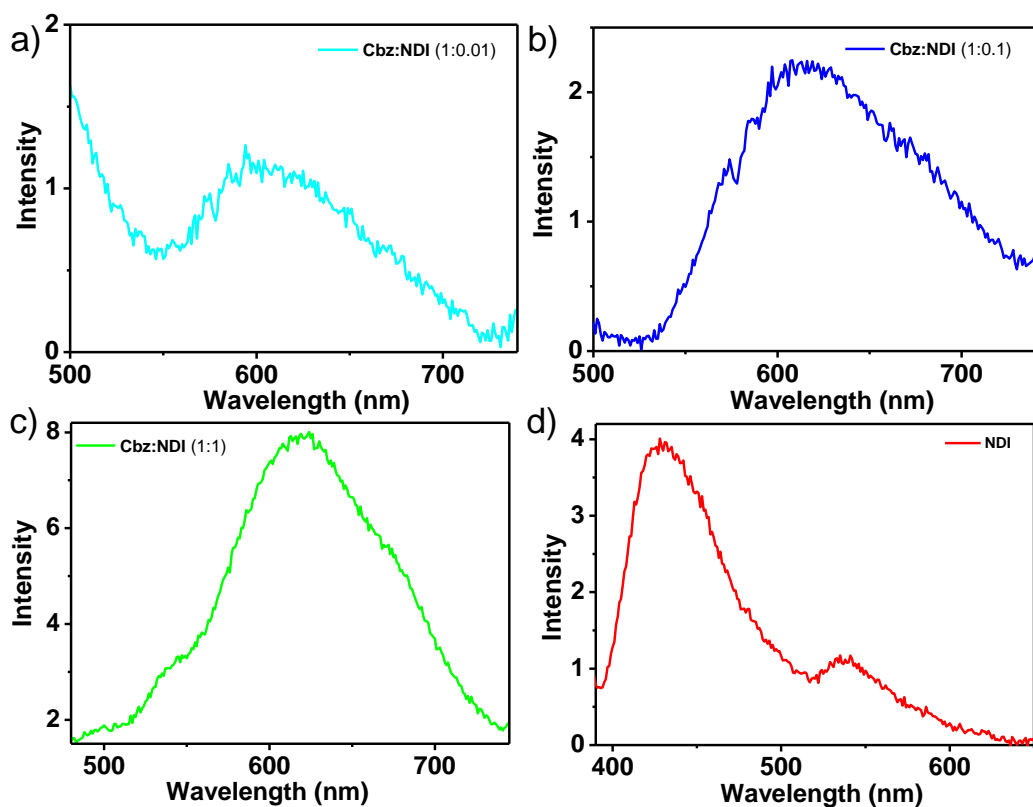
Figure S13. Phosphorescence spectra of **Cbz**:**NDI** with varying ratios a) 1:0.01, b) 1:0.1, c) 1: 1 and d) **NDI** in neat liquid thin film 25 $^{\circ}$C in air (λ_{ex} = 350 nm).
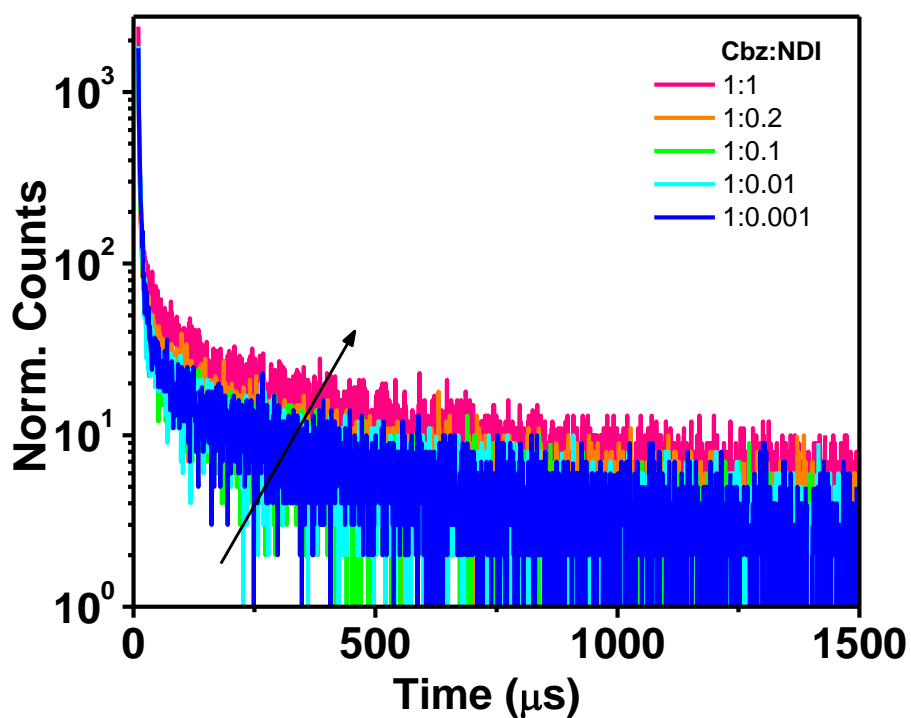
Figure S14. Variation of emission lifetime of RTPL emission of **Cbz:NDI** with an increasing equivalence of **NDI** in the neat liquid thin film (λ_{ex} = 374 nm, λ_{mon} = 620 nm).
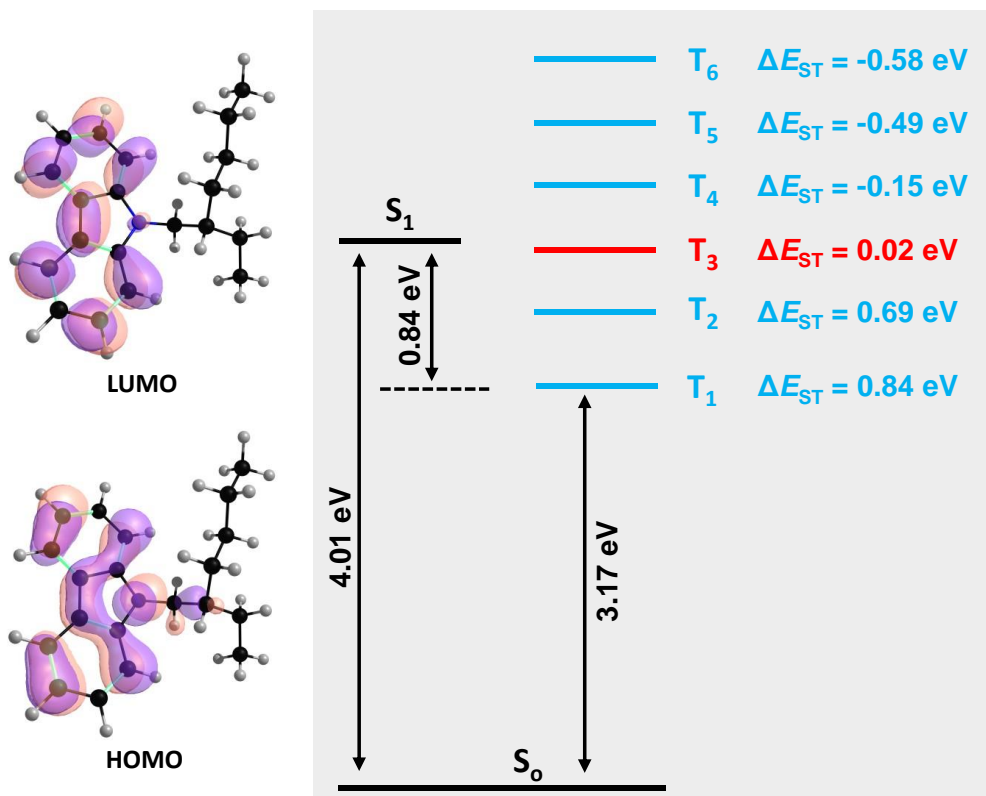
Figure S15. HOMO and LUMO of **Cbz** along with energy level diagram showing ΔE_{ST} from DFT calculations.
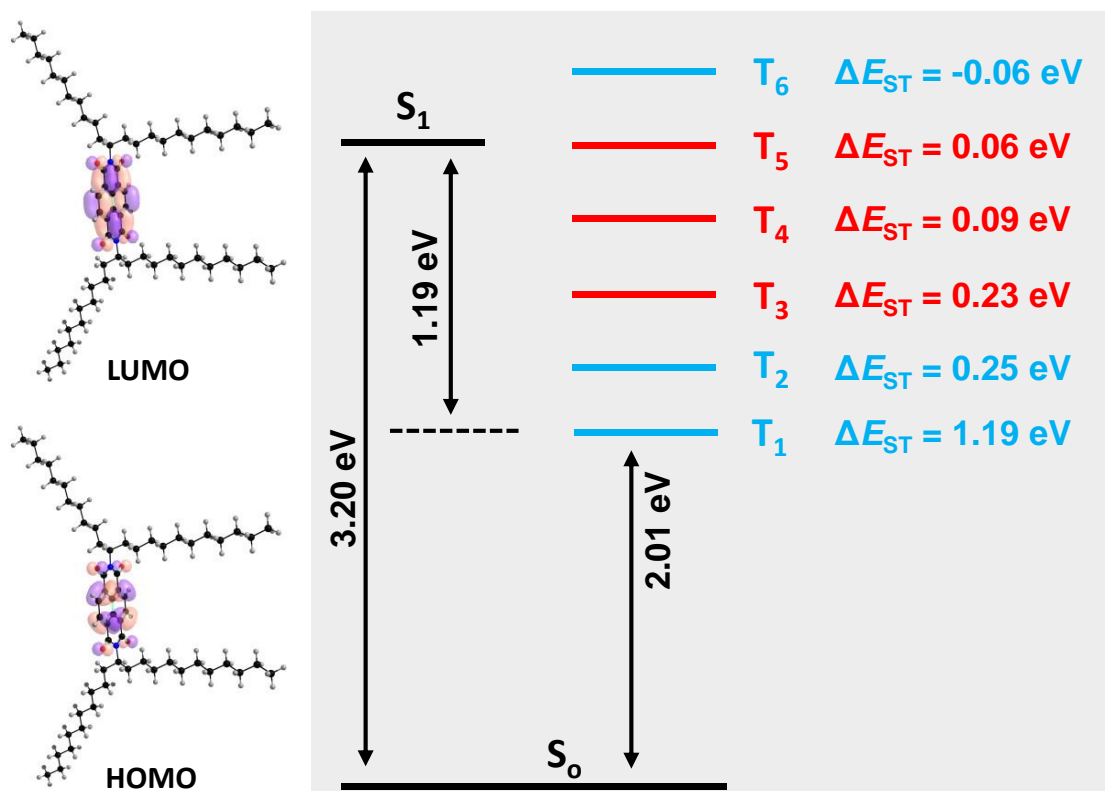
Figure S16. HOMO and LUMO of **NDI** along with energy level diagram showing ΔE_{ST} from DFT calculations.
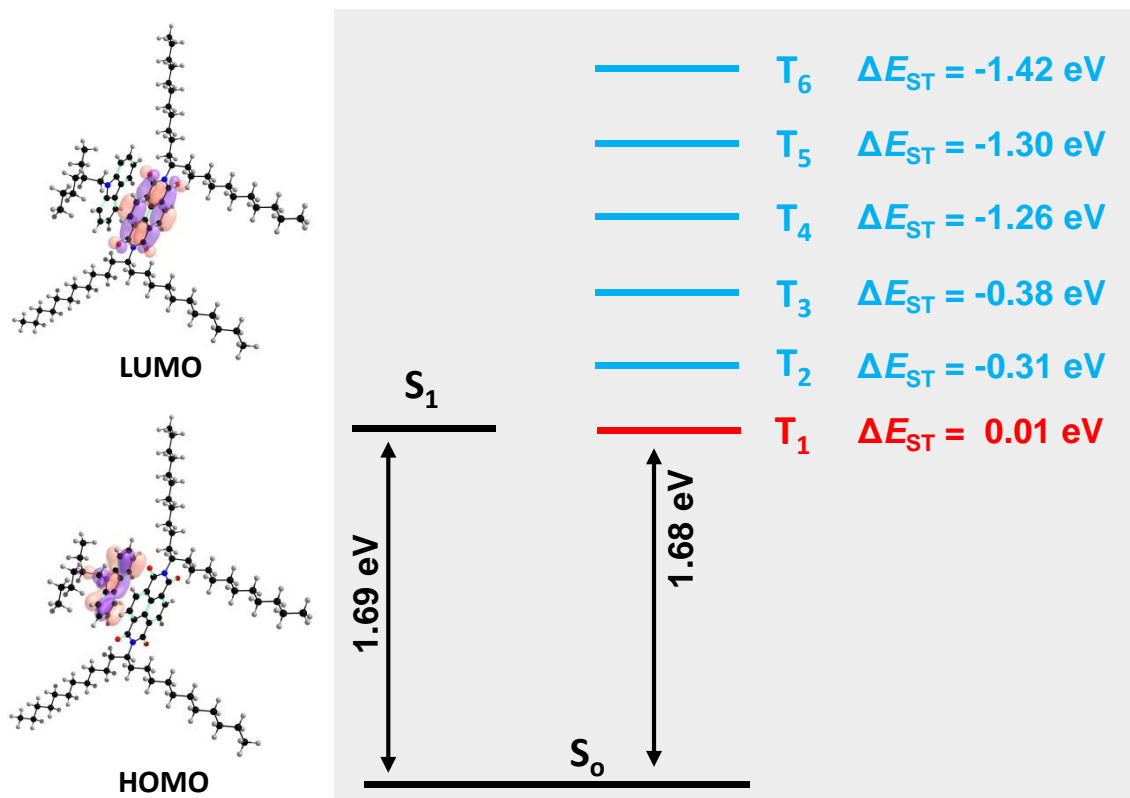
Figure S17. HOMO and LUMO of **Cbz:NDI** along with energy level diagram showing ΔE_{ST} from DFT calculations.
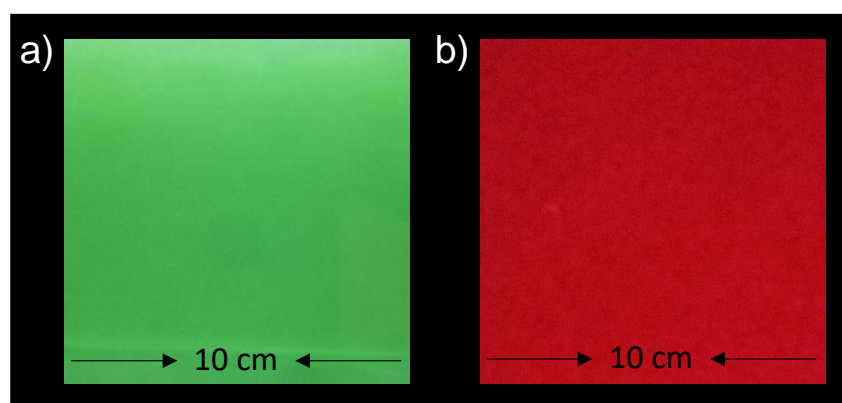
Figure S18. Photographs of a) **Cbz:NMI** (1:1) and b) **Cbz:NDI** (1:1) coated on glass (10x10 cm) under UV light (365 nm).
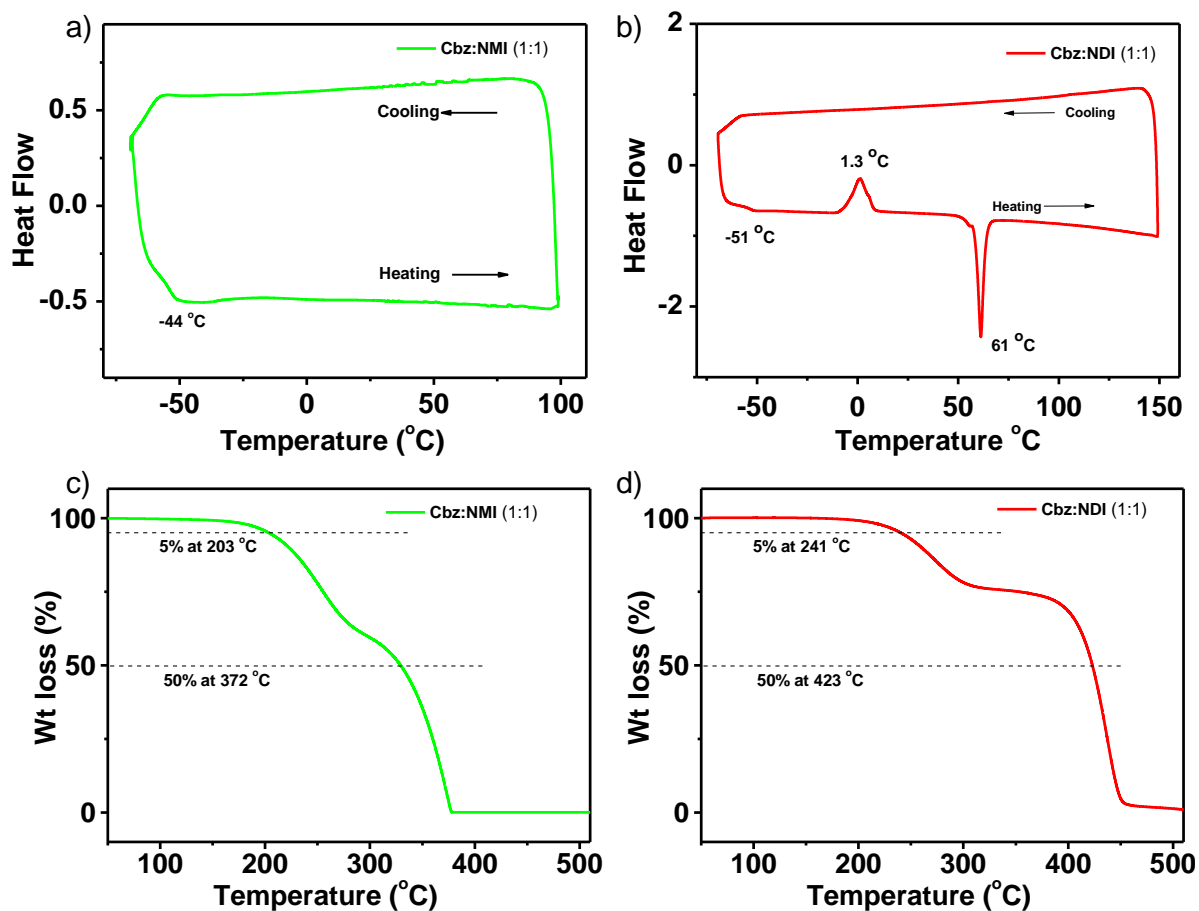
Figure S19. DSC thermograms in the heating trace at a scanning rate of 10 ˚C/min of a) **Cbz:NMI** (1:1), b) **Cbz:NDI** (1:1), and TGA of c) **Cbz:NMI** (1:1), d) **Cbz:NDI** (1:1).
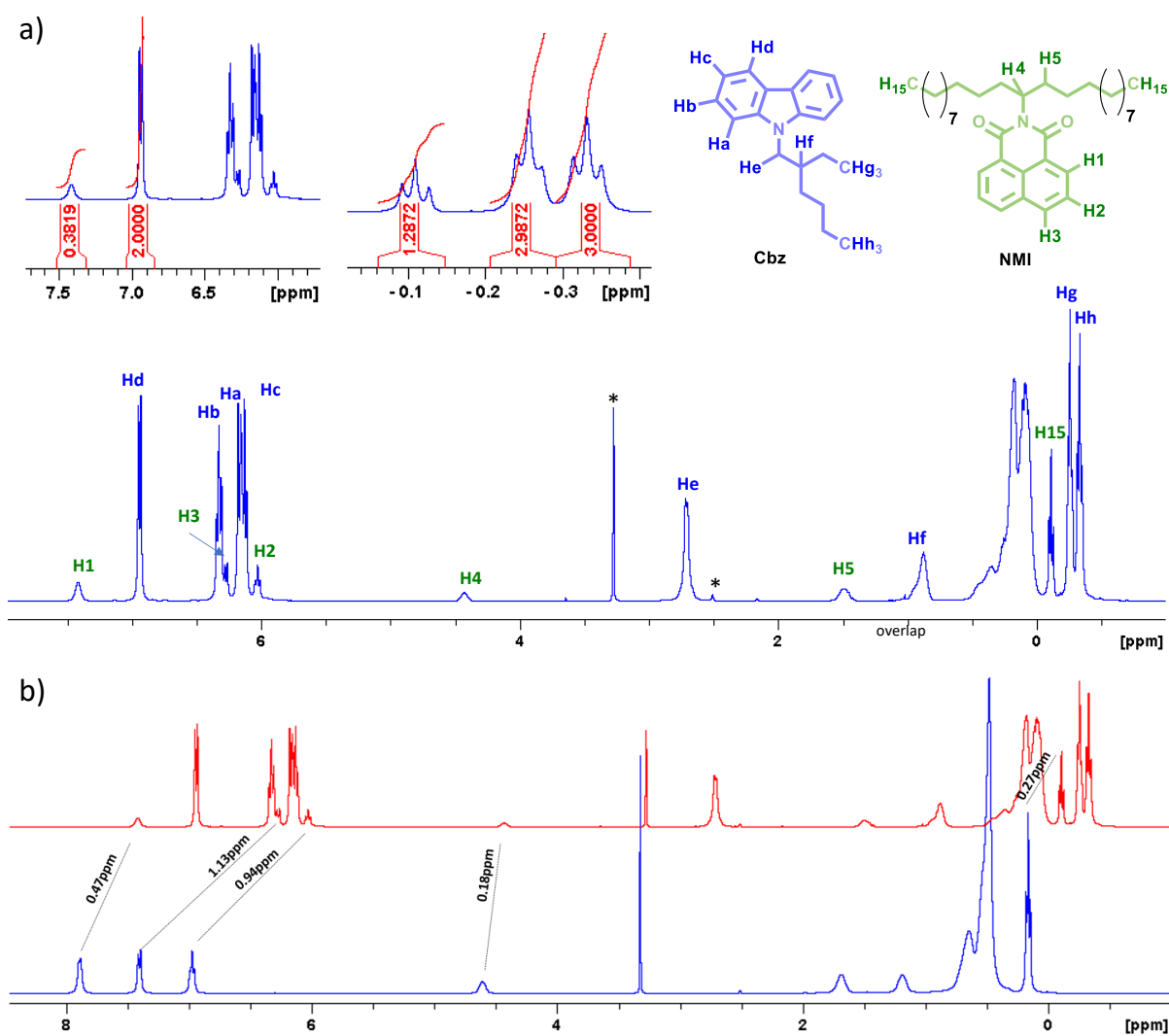
Figure S20. Chemical structures of **Cbz** and **NMI** with labelled protons and ^{1}H NMR spectrum of a) **Cbz:NMI** in the neat liquid at 318 K. Signal integration gives an estimate of the ratio, **Cbz:NMI** = 1:0.2. Asterisks indicate signals from the external lock solvent DMSO and residual water. b) Stack of **NMI** (blue) and **Cbz:NMI** (red) in the neat form at 318 K. Upfield shifts of **NMI** protons are indicated.
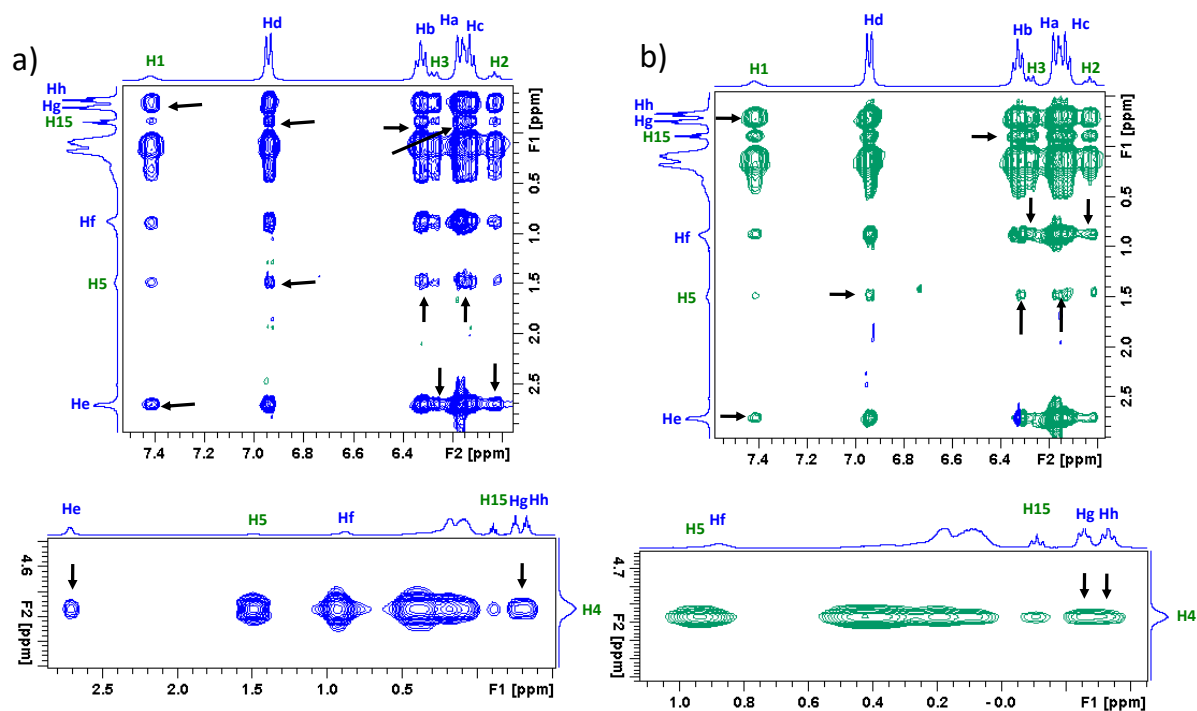
Figure S21. a) NOESY and b) ROESY spectra of **Cbz**:**NMI** (1:0.2) at 250 and 100 ms respectively, recorded at 318 K. Intermolecular cross-peaks are indicated by arrows.
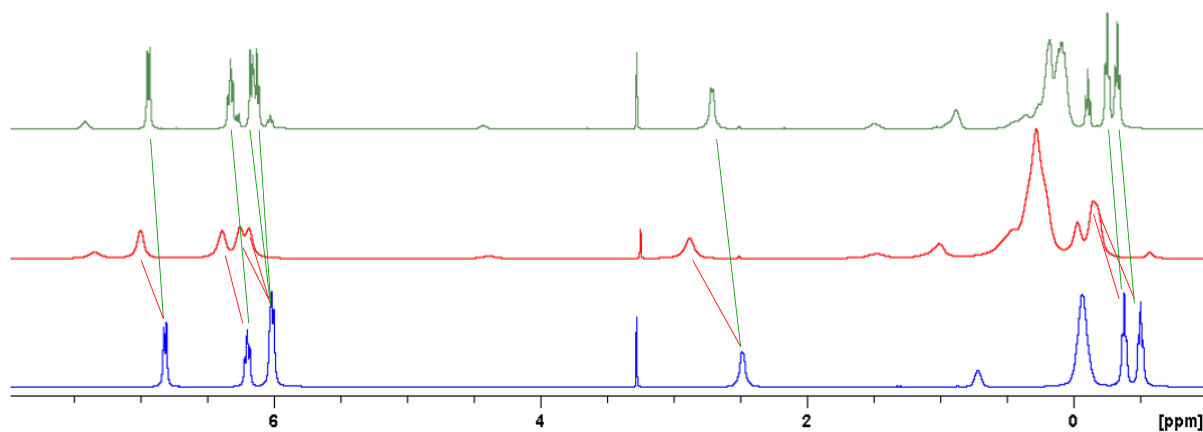
Figure S22. ^{1}H NMR spectra of **Cbz** (blue), **Cbz:NDI** (red) and **Cbz:NMI** (green) in the neat liquid at 318 K. Downfield shifts of **Cbz** protons in the complexes are indicated.
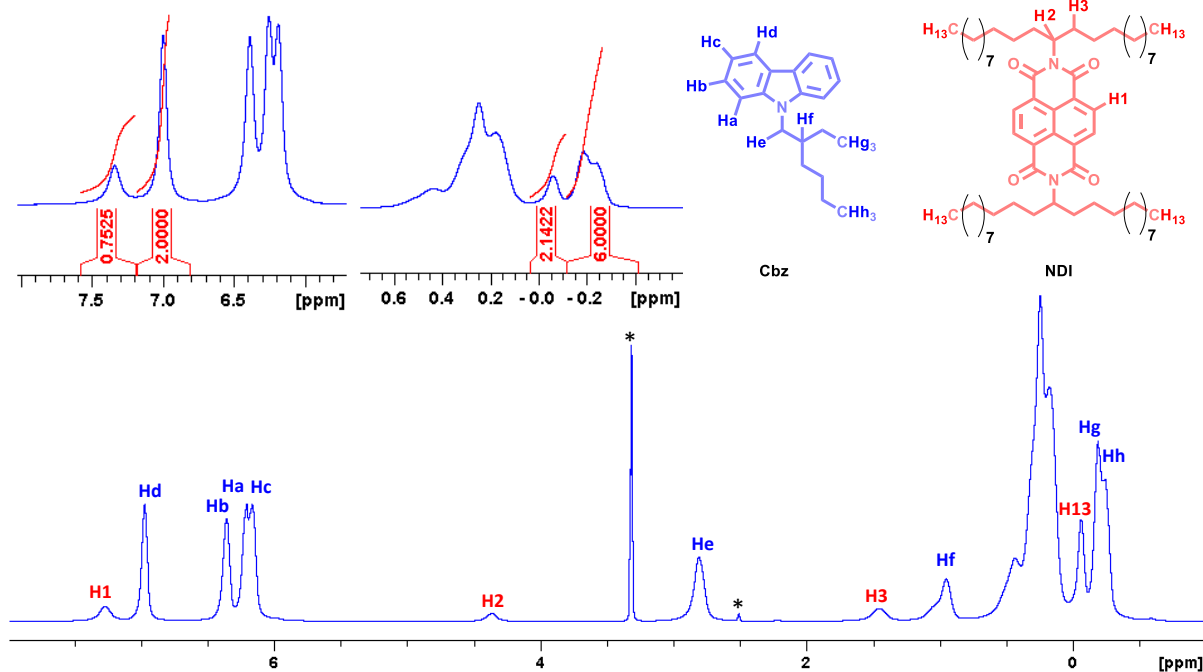
Figure S23. Chemical structures of **Cbz** and **NDI** with labelled protons and ^{1}H NMR spectrum of **Cbz:NDI** in the neat liquid at 318 K. Signal integration gives an estimate of the ratio, **Cbz:NDI** = 1:0.2. Asterisks indicate signals from the external lock solvent DMSO and residual water.
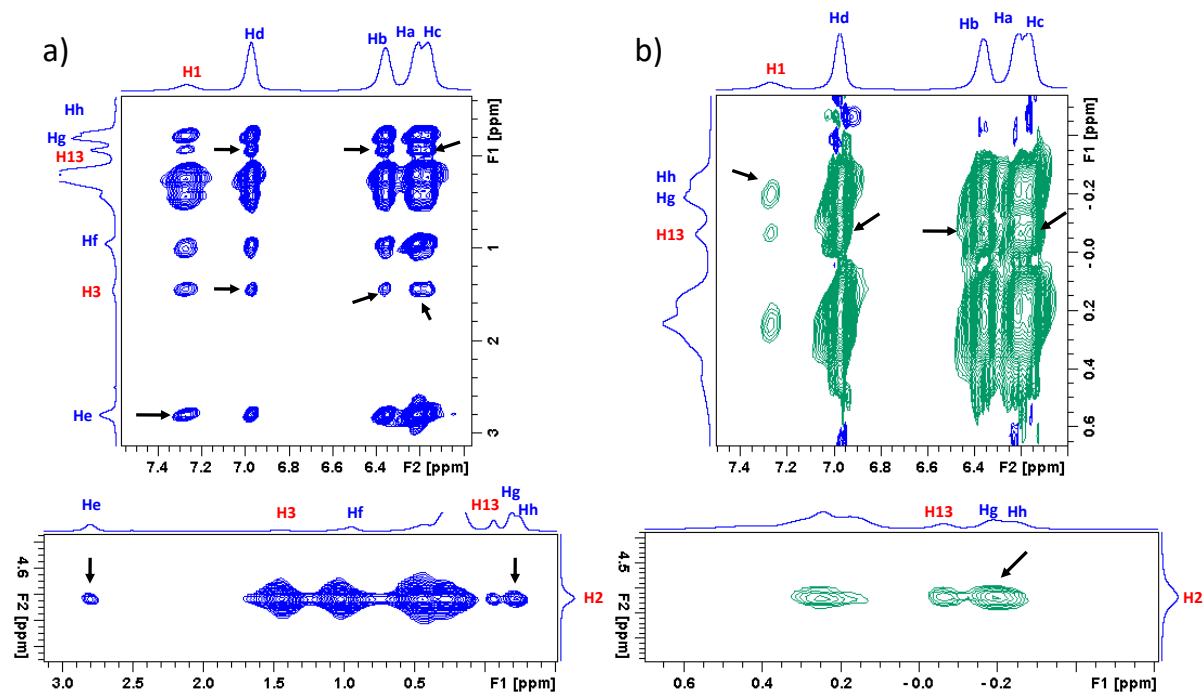
Figure S24. a) NOESY and b) ROESY spectra of **Cbz**:**NDI** (1:0.2) at 250 and 100 ms respectively, recorded at 318 K. Intermolecular cross-peaks are indicated by arrows.

Tables

Table S1. Emission lifetime of **Cbz**, **NMI** and **NDI** in dichloromethane ($C = 0.01$ mM, $l = 1$ mm, $\lambda_{ex} = 374$ nm).

Trials	Compounds	Wavelength monitored (nm)	Lifetime	CHISQ ($\chi2$) values
1	**Cbz**	390	$\tau_1 = 0.02$ ns (34 %) $\tau_2 = 0.94$ ns (48 %) $\tau_3 = 8.48$ ns (18 %)	1.16
2	**NMI**	410	$\tau_1 = 0.95$ ns (8 %) $\tau_2 = 6.04$ ns (92 %)	1.03
3	**NDI**	412	$\tau_1 = 0.89$ ns (86 %) $\tau_2 = 2.45$ ns (14 %)	1.14

Table S2. Emission lifetime of **Cbz**, **NMI**, and **NDI** in neat liquid thin-film ($\lambda_{ex} = 374$ nm).

Trials	Compounds	Wavelength monitored (nm)	Lifetime	CHISQ ($\chi2$) values
1	**Cbz**	410	$\tau_1 = 0.01$ ns (09%) $\tau_2 = 7.58$ ns (91 %)	0.98
2	**NMI**	468	$\tau_1 = 0.04$ ns (53 %) $\tau_2 = 1.30$ ns (10%) $\tau_3 = 13.7$ ns (37%)	1.21
3	**NDI**	490	$\tau_1 = 0.06$ ns (25%) $\tau_2 = 8.43$ ns (75%)	1.19

Table S3. Emission quantum yield of **Cbz**, **NMI**, **NDI**, **Cbz**:**NMI** (1:1), and **Cbz**:**NDI** (1:1) in solution and neat liquid.[S4]

Compounds	Quantum Yield (%)	
	Solution	**Neat liquid**
Cbz	3. 60%	11.34%
NMI	0.53 %	4.83%
NDI	0.25 %	1.44%
Cbz:NMI (1:1)	2.38 %	7.05%
Cbz:NDI (1:1)	1.38 %	2.37%

Table S4. Variation of emission lifetime of **Cbz:NMI** with an increasing equivalence of **NMI** in the neat liquid thin film (λ_{ex} = 374 nm, λ_{mon} = 495 nm).

Trials	Cbz:NMI	Lifetime (ns)	CHISQ (χ2) values
1	1:0.001	τ_1 = 0.02 (28%) τ_2 = 2.68 (14%) τ_3 = 16.6 (58%)	1.25
2	1:0.01	τ_1 = 0.04 (38%) τ_2 = 2.85 (14%) τ_3 = 18.0 (48%)	1.16
3	1:0.1	τ_1 = 0.04 (45%) τ_2 = 4.31 (12%) τ_3 = 21.6 (43%)	1.16
4	1:0.2	τ_1 = 0.09 (04%) τ_2 = 5.82 (30%) τ_3 = 22.5 (66%)	1.04
5	1:1	τ_1 = 2.18 (07%) τ_2 = 10.0 (42%) τ_3 = 26.0 (51%)	1.11

Table S5. Variation of emission lifetime of RTPL emission of **Cbz:NDI** with an increasing equivalence of **NDI** in the neat liquid thin film (λ_{ex} = 374 nm, λ_{mon} = 620 nm).

Trials	Cbz:NDI	Lifetime (μs)	CHISQ (χ2) values
1	1:0.001	τ_1 = 2.07 (30%) τ_3 = 21.9 (17%) τ_2 = 326 (53%)	1.22
2	1:0.01	τ_1 = 2.16 (30%) τ_3 = 24.2 (18%) τ_2 = 391 (52%)	1.10
3	1:0.1	τ_1 = 1.57 (19%) τ_2 = 29.0 (19%) τ_3 = 410 (62%)	1.12
4	1:0.2	τ_1 = 2.44 (33%) τ_3 = 42.3 (17%) τ_2 = 434 (50%)	1.11
5	1:1	τ_1 = 1.05 (12%) τ_2 = 31.4 (18%) τ_3 = 485 (70%)	1.01

Details of DFT calculations

Ground (S0) state calculations were performed using restricted density functional theory (DFT). Singlet and triplet excited states were investigated using time-dependent density functional theory (TDDFT). The ground state singlet (S_0) state was calculated using B3LYP/6-31G(d) level of theory. Also the TDDFT calculations were done with same level of theory. All the geometries of the complexes in the S_0 state were optimized. The optimized Cartesian coordinates and total energies are listed below. On the basis of the Frank-Condon principle, the absorption properties were evaluated using the optimized S_0 state structure. The Gaussian09[S5] software was used in all the DFT and TDDFT calculations.

Optimized Cartesian coordinates of different complexes (S_0 state) at the B3LYP/6-31G(d) level of theory.

Cbz
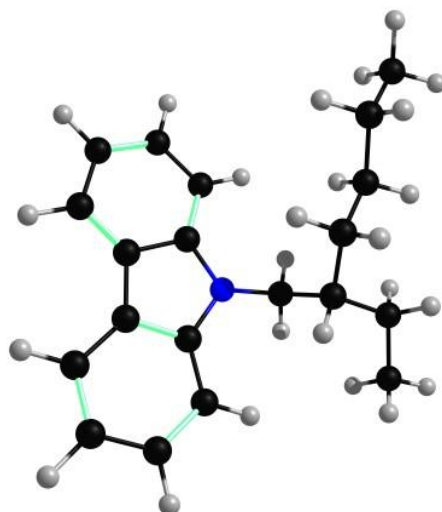
Table S6. π-π* Excitation properties of Cbz calculated at the TD-B3LYP/6-31G(d) level

	ΔE (eV)	λ (nm)	f	Configuration (orbital symmetry)	Coefficient
S0 _ S1	4.0079	309.35	0.0371	HOMO (76) _ LUMO (77)	0.68097
S0 _ S2	4.5139	274.67	0.0772	HOMO-1 (75)_LUMO (77)	0.58613
S0 _ S3	5.2125	237.86	0.4419	HOMO (76)_LUMO+1 (78)	0.53357
S0 _ S4	5.3279	232.71	0.0209	HOMO-1 (75)_LUMO+1 (78)	0.57355
S0 _ S5	5.4281	228.41	0.1577	HOMO-2 (74)_LUMO (77)	0.58559
S0 _ S6	5.8230	212.92	0.1809	HOMO (76)_LUMO+2 (79)	0.1809
S0 _ S7	5.9311	209.04	0.3967	HOMO (76)_LUMO+3(80)	0.55531

	ΔE (eV)	λ (nm)	f	Configuration (orbital symmetry)	Coefficient
S0 _ S8	6.2123	199.58	0.0711	HOMO-1 (75)_LUMO+3(80)	0.39414
S0 _ S9	6.2588	198.10	0.0428	HOMO-1 (75)_LUMO+2 (79)	0.42909
S0 _ S10	6.3991	193.75	0.0163	HOMO-2 (74)_LUMO+1 (78)	0.52360

	ΔE (eV)	λ (nm)	f	Configuration (orbital symmetry)	Coefficient
S0 _ T1	3.1710	390.99	0.0000	HOMO-1 (75) _ LUMO (77)	0.60607
S0 _ T2	3.3183	3.3183	0.0000	HOMO (76)_LUMO (77)	0.68280
S0 _ T3	3.9901	310.73	0.0000	HOMO (76)_LUMO+1 (78)	0.55781
S0 _ T4	4.1608	297.98	0.0000	HOMO (76)_LUMO+3 (79)	0.47200
S0 _ T5	4.5037	275.30	0.0000	HOMO-1 (75)_LUMO+1 (78)	0.64650
S0 _ T6	4.5868	270.31	0.0000	HOMO-2 (74)_LUMO (77)	0.53909
S0 _ T7	4.8498	255.65	0.0000	HOMO (76)_LUMO+2 (79)	0.40726
S0 _ T8	5.1541	240.56	0.0000	HOMO-1(75)_LUMO+2 (79)	0.62672
S0 _ T9	5.4074	229.29	0.0000	HOMO (76)_LUMO+3 (80)	0.59749
S0 _ T10	5.6244	220.44	0.0000	HOMO-2(74)_LUMO+1 (78)	0.55549

NDI
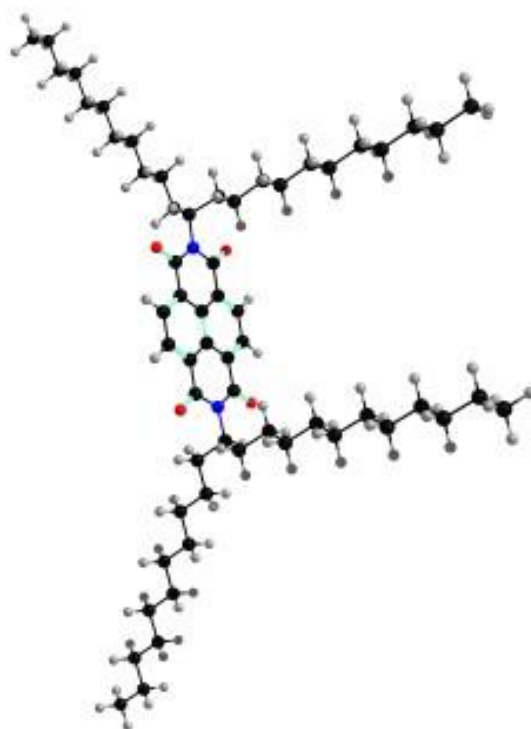
Table S7. π-π* Excitation properties of NDI calculated at the TD-B3LYP/6-31G(d) level

	ΔE (eV)	λ (nm)	f	Configuration (orbital symmetry)	Coefficient
S0 _ S1	3.2081	386.47	0.0008	HOMO (250) _ LUMO (253)	0.65258
S0 _ S2	3.3578	369.24	0.3956	HOMO (252) _ LUMO (253)	0.69924
S0 _ S3	3.3693	367.98	0.0001	HOMO (248) _ LUMO (253)	0.68979
S0 _ S4	3.4280	361.68	0.0002	HOMO (247) _ LUMO (253)	0.66751
S0 _ S5	3.5371	350.53	0.0000	HOMO (251) _ LUMO (253)	0.62916
S0 _ S6	3.5724	347.06	0.0000	HOMO (249) _ LUMO (253)	0.67813
S0 _ S7	3.6119	343.27	0.0001	HOMO (245) _ LUMO (253)	0.65995
S0 _ S8	3.9095	317.13	0.0753	HOMO (246) _ LUMO (253)	0.63910
S0 _ S9	4.2670	290.57	0.0000	HOMO (244) _ LUMO (253)	0.67794
S0 _ S10	4.2741	290.09	0.0069	HOMO (243) _ LUMO (253)	0.65370

	ΔE (eV)	λ (nm)	f	Configuration (orbital symmetry)	Coefficient
S0 _ T1	2.0136	615.72	0.0000	HOMO (252) _ LUMO (253)	0.69372

S0 _ T2	2.9535	419.79	0.0000	HOMO (251) _ LUMO (253)	0.60324
S0 _ T3	2.9758	416.64	0.0000	HOMO (250) _ LUMO (253)	0.66972
S0 _ T4	3.1165	397.83	0.0000	HOMO (248) _ LUMO (253)	0.65445
S0 _ T5	3.1408	394.75	0.0000	HOMO (249) _ LUMO (253)	0.61594
S0 _ T6	3.2087	386.40	0.0000	HOMO (247) _ LUMO (253)	0.66218
S0 _ T7	3.2571	380.66	0.0000	HOMO (246) _ LUMO (253)	0.56540
S0 _ T8	3.3737	367.50	0.0000	HOMO (245) _ LUMO (253)	0.63956
S0 _ T9	3.4467	359.72	0.0000	HOMO (252) _ LUMO (254)	0.43604
S0 _ T10	4.2079	294.65	0.0000	HOMO (243) _ LUMO (253)	0.52034

Cbz:NDI
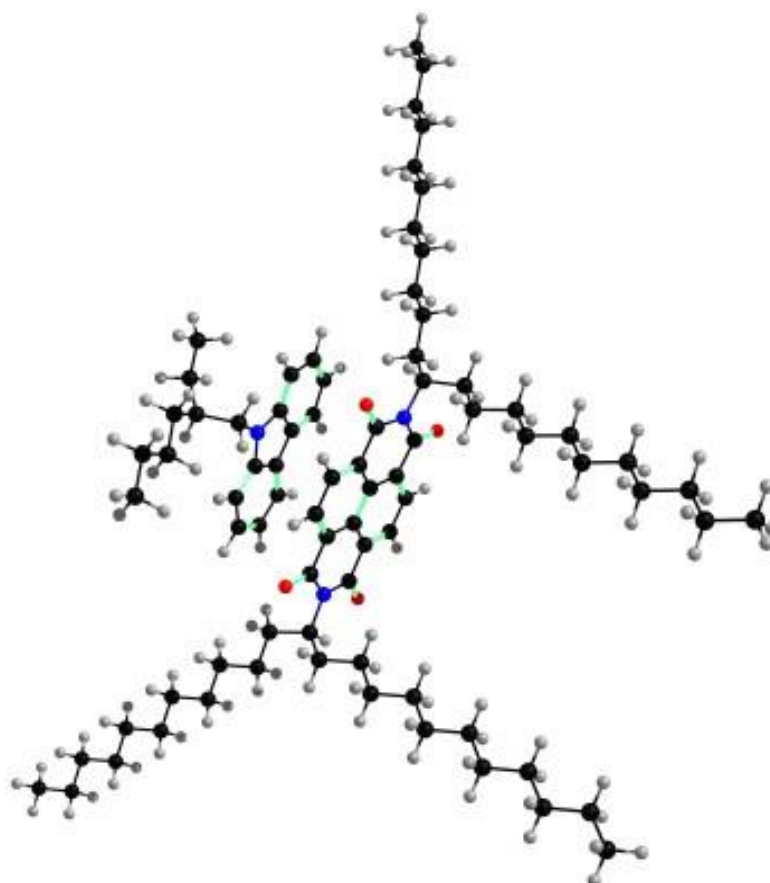
Table S8. π-π* Excitation properties of Cbz:NDI calculated at the TD-B3LYP/6-31G(d) level

	Δ*E* (eV)	*λ* (nm)	*f*	Configuration (orbital symmetry)	Coefficient

S0 _ S1	1.6934	732.17	0.0006	HOMO (328) _ LUMO (329)	0.70678
S0 _ S2	2.0739	597.82	0.0007	HOMO-1 (327) _ LUMO (329)	0.70689
S0 _ S3	3.1019	399.70	0.0218	HOMO-2 (326) _ LUMO (329)	0.53696
S0 _ S4	3.2229	384.69	0.0001	HOMO-5 (323) _ LUMO (329)	0.68545
S0 _ S5	3.3486	370.26	0.2472	HOMO-3 (325) _ LUMO (329)	0.51994
S0 _ S6	3.3863	366.14	0.0153	HOMO-7 (321) _ LUMO (329)	0.66635
S0 _ S7	3.4446	359.93	0.0014	HOMO-8 (320) _ LUMO (329)	0.54382
S0 _ S8	3.4471	359.68	0.0004	HOMO (328) _ LUMO+1 (330)	0.61341
S0 _ S9	3.5389	350.35	0.0002	HOMO-4 (324) _ LUMO (329)	0.63220
S0 _ S10	3.5937	345.00	0.0004	HOMO-6 (322) _ LUMO (329)	0.66284

	ΔE (eV)	λ (nm)	f	Configuration (orbital symmetry)	Coefficient
S0 _ T1	1.6848	735.90	0.0000	HOMO (328) _ LUMO (329)	0.70172
S0 _ T2	2.0032	618.94	0.0000	HOMO-2 (326) _ LUMO (329)	0.58339
S0 _ T3	2.0742	597.75	0.0000	HOMO-1 (327) _ LUMO (329)	0.69333
S0 _ T4	2.9534	419.80	0.0000	HOMO-4 (324) _ LUMO (329)	0.57144
S0 _ T5	2.9896	414.71	0.0000	HOMO-5 (323) _ LUMO (329)	0.65839
S0 _ T6	3.1151	398.01	0.0000	HOMO-3 (325) _ LUMO (329)	0.55109
S0 _ T7	3.1338	395.64	0.0000	HOMO-7 (321) _ LUMO (329)	0.65152
S0 _ T8	3.1570	392.73	0.0000	HOMO-6 (322) _ LUMO (329)	0.56033
S0 _ T9	3.1708	391.02	0.0000	HOMO-1 (327) _ LUMO+4 (333)	0.52731
S0 _ T10	3.2309	383.75	0.0000	HOMO-8 (320) _ LUMO (329)	0.65055

References

S1. Justyniarski, A.; Zaręba, J. K.; Hańczyc, P.; Fita, P.; Chołuj, M.; Zaleśny, R.; Samoc, M.; *J. Mater. Chem. C*, **2018**, *6*, 4384.

S2. Wakchaure, V. C.; Goudappagouda, Das, T.; Ravindranathan, S.; Babu, S. S., *Nanoscale*, **2021**, *13*, 10780-10784.

S3. Wakchaure, V. C.; Pillai, L. V.; Goudappagouda, Ranjeesh, K. C.; Chakrabarty, S.; Ravindranathan, S.; Rajamohanan, P. R., Babu, S. S., *Chem. Commun.*, **2019**, *55*, 9371-9374.

S4. a) Goudappagouda, A. Manthanath, V. C. Wakchaure, K. C. Ranjeesh, T. Das, K. Vanka, T. Nakanishi, S. S. Babu, *Angew. Chem., Int. Ed.*, **2019**, *58*, 2284-2288; b) M. Komura, T. Ogawa, Y. Tani, *Chem. Sci.*, **2021**, *12*, 14363-14368.

S5. Gaussian 09, Revision E.01; M. J. Frisch, G. W. Trucks, H. B. Schlegel, G. E. Scuseria, M. A. Robb, J. R. Cheeseman, G. Scalmani, V. Barone, B. Mennucci, G. A. Petersson, H. Nakatsuji, M. Caricato, X. Li, H. P. Hratchian, A. F. Izmaylov, J. Bloino, G. Zheng, J. L. Sonnenberg, M. Hada, M. Ehara, K. Toyota, R. Fukuda, J. Hasegawa, M. Ishida, T. Nakajima, Y. Honda, O. Kitao, H. Nakai, T. Vreven, J. A. Montgomery, Jr., J. E. Peralta, F. Ogliaro, M. Bearpark, J. J. E. Heyd, K. N. B. Kudin, V. N. Staroverov, R. Kobayashi, J. K. Raghavachari, A. Rendell, J. C. Burant, S. S. Iyengar, J. Tomasi, M. Cossi, N. Rega, J. M. Millam, M. Klene, J. E. Knox, J. B. Cross, V. Bakken, C. Adamo, J. Jaramillo, R. Gomperts, R. E. Stratmann, O. Yazyev, A. J. Austin, R. Cammi, C. Pomelli, J. W. Ochterski, R. L. Martin, K. Morokuma, V. G. Zakrzewski, G. A. Voth, P. Salvador, J. J. Dannenberg, S. Dapprich, A. D. Daniels, Ö. Farkas, J. B. Foresman, J. V. Ortiz, J. Cioslowski, D. J. Fox, Gaussian, Inc., *Wallingford CT*, **2009**.